*Supporting information*

# Efficient Synthesis of Apremilast Precursor and Chiral β-Hydroxy Sulfones via Ketoreductase-Catalyzed Asymmetric Reduction

*Jiyang Gu[a], Xiao Gao[a], Dong Qian[a], Huibin Wang[a], Xian Jia[b], Wenhe Zhang*[a], Bin Qin*[c], and Song You*[a]*

[a]School of Life Sciences and Biopharmaceutical Sciences, Shenyang Pharmaceutical University, 103 Wenhua Road, Shenhe, Shenyang 110016, People's Republic of China

[b]School of Pharmaceutical Engineering, Shenyang Pharmaceutical University, 103 Wenhua Road, Shenhe, Shenyang 110016, People's Republic of China

[c]Wuya College of Innovation, Shenyang Pharmaceutical University, 103 Wenhua Road, Shenhe, Shenyang 110016, People's Republic of China

*Corresponding author: yousong207@163.com (S.Y.); to-qinbin@163.com (B.Q.); zhangwenhe306@163.com (W.Z.)

## Contents

## Supporting Materials and Methods

### General chemicals and equipment

Unless otherwise specified, all chemical or molecular biological reagents and solvent were purchased from commercial sources and used as received. Achiral GC analysis was conducted with SCION 456-GC (SCION Instruments) system. Achiral HPLC analysis was conducted with Hitachi-Primaide system and chiral HPLC analysis was performed on a JASCO LC-1500 system using chiral columns (Daicel Chiral Technologies Co., LTD, Shanghai, China) with a JASCO UV-2075 detector. $^{1}$H NMR (400 MHz) spectra were recorded using a Bruker AVANCE-400 in $CDCl_3$ with TMS as an internal standard.

### Expression of KREDs

All the KREDs and mutants were cloned from our previous studies on SDR-catalyzed asymmetric reduction of halogen-substituted acetophenones (Table S1).[1, 2] The expression of KREDs were performed following standard procedures: recombinant *E. coli BL21*(DE3) cells harboring the gene of KRED was cultured in 1 L LB medium containing 100 μg mL$^{-1}$ kanamycin or ampicillin at 220 rpm, 37 ℃. When OD600 arrived at 0.8-1.0, the cells were induced by adding 0.1 mM IPTG (isopropyl β-D-1-thiogalactopyranoside) at 220 rpm, 18 °C for 20 h. Finally, the culture medium was centrifugated at 3000 rpm for 10 min and the cells were harvested by removing the supernatant. The harvested pellets were stored at -20°C until further use.

**Table S1. The NCBI accessions of wild-type KREDs in this study.**

| KREDs | NCBI Accession | reference |
|---|---|---|
| BmSDR5-WT | WP_015638890 | [2] |
| BmSDR11-WT | WP_015638890 | [2] |
| BsSDR13-WT | WP_044429803.1 | [2] |
| LfSDR1-WT | WP_015638890 | [2] |
| CgKR1-WT | XP_445913 | [1] |

**General procedure for synthesis of β-keto sulfones**

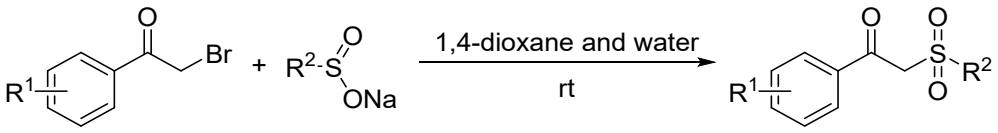


Except that **1a**, **1j**, **1k**, and **1l** were purchased from commercial sources, others were synthesized following standard procedures[3]: Bromoacetophenone (1g, 5.0 mmol) was added to a 100 mL flask, and then 20 mL 1,4-dioxane was added to dissolve it. Then 20 mL water solution of sodium methylene sulfite or sodium phenylsulfite was added to the flask, and it was stirred at room temperature. The reaction was monitored by TLC until the end of the reaction. 1,4-Dioxane in the reaction system was removed by rotary evaporator, then a small amount of water was added, and then it was extracted by ethyl acetate. The combined organic layers were concentrated in vacuo, and the resulting residue was stirred with mixtures of petroleum ether and EtOAc (petroleum ether:EtOAc = 10:1) at room temperature, then it was filtered to give precipitates as solid. Finally, the ketones obtained reacted with $NaBH_4$ giving racemic β-hydroxy sulfones.

**Asymmetric reduction of substrates 1a-1t at analytical scale**

The asymmetric reduction of substrates **1a-1t** was carried out using a NAD(P)H recycling system. Substrates (20 mM final) in 100 μL DMSO, glucose (9.0 mg, 50 mM), and $NADP^+$ (0.2 mg, 0.27 mM) were added to the supernatant of the enzymes' lysate (prepared by the mixture of 100 mg wet cells of *E. coli* Rosetta2 DE3 harboring a KRED and 20 mg wet cells of *E. coli* Rosetta2 DE3 harboring GDH using sonication) in 900 μL PBS buffer (100 mM, pH 7.0). The reaction was performed at 220 rpm and 30 ℃ for 12 h, and then extracted with EtOAc (2 × 1 mL). The combined organic layers were concentrated in vacuo. The product was analyzed by achiral HPLC or GC for conversion and chiral HPLC for *ee* values.

**Gram-scale Synthesis of (*R*)-2a**

The reaction was carried out on a 20 mL scale with the substrate concentration of 50 g/L (soluble in 3 mL DMSO firstly), the supernatant of the enzymes' lysate (prepared by the mixture of 100 mg wet cells of *E. coli* Rosetta2 DE3 harboring a KRED and 20 mg wet cells of *E. coli* Rosetta2 DE3 harboring GDH using sonication), glucose (1.65 g, 2.5 equiv.) and $NADP^+$ (4 mg, 0.27 mM) in PBS buffer (100 mM, pH 7.0). The reaction was performed at 30 °C and 220 rpm and kept the solution at pH 7.0 by adding 2 M $Na_2CO_3$ aqueous solution. After 12 h, the reaction system was extracted with ethyl acetate and concentrated in vacuo, and then purified by flash chromatography (silica gel, petroleum ether:EtOAc = 2:1), affording (*R*)-**1a** as a white solid.

**Kinetic assay**

Kinetic analysis was carried out using a microplate spectrophotometer (Epoch, BioTek) by measuring the consumption of NADPH (λ = 340 nm). Assays were performed in 200 μL PBS buffer (100 mM, pH 7.0) with 0.2 mM NADPH and using purified protein with an appropriate concentration at substrate concentrations ranging from 0.05 mM to 1.0 mM at 30 °C. The extinction coefficient for NADPH under the assay conditions was used as 6220 $M^{-1}$ $cm^{-1}$. All assays were repeated in triplicate. The kinetic parameters were calculated by nonlinear regression according to the Michaelis−Menten equation.

**Methods for the measurement of conversion**

The conversion was determined by achiral GC or HPLC with two methods below, and retention times for substrates and products were shown as Table S2.

**Method A**

Achiral GC analysis for the measurement of conversion was conducted with SCION 456-GC (SCION Instruments) system. a Rtx®-5 capillary column (0.32 mm × 30 m, 0.25 μm film thickness; Restek) was used. The injector temperature was kept at 250 °C and the detector at 280 °C. The column temperature was held at 60 °C for 0.5 min, increased to 290 °C at a rate of 25 °C $min^{-1}$, and then kept 290 °C for 1.5 min.

**Method B**

Achiral HPLC analysis for the measurement of conversion was conducted with Hitachi-Primaide system on C18 column, 254 nm, acetonitrile: $H_2O$ = 40:60; flow 1.0 mL/min.

**Table S2. Achiral GC or HPLP methods for measurement of conversion**

| Substrate | Method | Rt (Sub.) min | Rt (Prod.) min | Substrate | Method | Rt (Sub.) min | Rt (Prod.) min |
|---|---|---|---|---|---|---|---|
| **1a** | **A** | 8.8 | 9.0 | **1k** | **A** | 7.1 | 7.3 |
| **1b** | **A** | 7.0 | 7.3 | **1l** | **A** | 9.1 | 9.2 |
| **1c** | **A** | 7.5 | 7.7 | **1m** | **B** | 15.0 | 10.5 |
| **1d** | **A** | 8.0 | 8.3 | **1n** | **A** | 9.8 | 9.09 |
| **1e** | **A** | 8.2 | 8.4 | **1o** | **A** | 9.8 | 10.0 |
| **1f** | **A** | 6.9 | 7.3 | **1p** | **B** | 10.9 | 7.3 |
| **1g** | **A** | 7.7 | 8.1 | **1q** | **A** | 9.0 | 9.1 |
| **1h** | **A** | 7.7 | 8.1 | **1r** | **A** | 9.7 | 9.9 |
| **1i** | **A** | 8.2 | 8.6 | **1s** | **A** | 9.7 | 9.9 |
| **1j** | **A** | 6.5 | 6.7 | **1t** | **A** | 10.1 | 10.4 |

**Identification of the absolute configuration of product**

The absolute configurations were identified by comparing optical rotation ($[\alpha]_D^{20}$ ($c$=0.01, $CHCl_3$)) of products obtained by CgKR1-catalyzed asymmetric reduction with literature data[3-6] (Table S3).

**Table S3. The absolute configurations, *ee* and $[\alpha]_D^{20}$ of products obtained by CgKR1-catalyzed asymmetric reduction**

| Product | *ee* (%) | $[\alpha]_D^{20}$ | Config [Ref] | Product | *ee* (%) | $[\alpha]_D^{20}$ | Config [Ref] |
|---|---|---|---|---|---|---|---|
| **2a** | 99.8 | +51.6 | *S* [4] | **2k** | 99.9 | +16.0 | *S* [6] |
| **2b** | 99.8 | +51.6 | *S* [3] | **2l** | 99.9 | +24.4 | *S* [3] |
| **2c** | 94.8 | +46.1 | *S* [3] | **2m** | 96.0 | +24.1 | *S* [3] |
| **2d** | 99.3 | +48.0 | *S* [a] | **2n** | 99.9 | +33.1 | *S* [3] |
| **2e** | 99.2 | +39.4 | *S* [3] | **2o** | 99.7 | +17.5 | *S* [3] |
| **2f** | 99.9 | +47.7 | *S* [a] | **2p** | 99.9 | +21.0 | *S* [3] |
| **2g** | 99.9 | +48.1 | *S* [a] | **2q** | 99.9 | +22.4 | *S* [3] |

| | | | | | | | |
|---|---|---|---|---|---|---|---|
| **2h** | 99.9 | +47.1 | *S* [3] | **2r** | 99.9 | +17.5 | *S* [a] |
| **2i** | 99.9 | +36.0 | *S* [a] | **2s** | 99.7 | +14.0 | *S* [3] |
| **2j** | 99.9 | +21.6 | *S* [5] | **2t** | 99.9 | +13.7 | *S* [3] |

[a]The absolute configuration were assigned by analogy.

**Molecular simulations**

The model structures of LfSDR1-V186A/E141I and CgKR1-F92I were constructed based on homology modeling methods and the models were created using Swiss-Model server[7] using 1ZK4[8] (PDB ID) and 4PVD[9] as corresponding template. Docking calculations were performed using AutoDock program.[10] For the docking algorithm of LfSDR1-V186A/E141I variant, the ligand and residues Tyr152 was set as flexibility while the other of protein was set as rigid. And the grid box dimensions and center were set as follows: center x, y, z = 10.872, 10.614, 11.834, size x, y, z = 16, 16, 16. For the docking algorithm of CgKR1-F92I, the ligand and residues Tyr175, Ser134 were set as flexibility while the other of protein were set as rigid and the grid box dimensions and center were set as follows: center x, y, z = 19.898, 8.897, 112.426, size x, y, z = 20, 20, 20.

The obtained Pro*R* and Pro*S* models of two KREDs were subjected to molecular dynamic (MD) simulation. Desmond/Maestro (Non-Commercial Distribution, Version 2019.2)[11] was employed for MD simulation. After protein preparation, each enzyme-substrate system was immersed in an orthorhombic box of SPC waters, while the distances for the orthorhombic box were set to 7.0 Å (a, b, and c) and the ionic strength of the NaCl was set to 0.15 M. In the MD simulations, the enzyme-substrate system was described by the OPLS_2005 force field. An NVT ensemble, a temperature of 300 K, a total simulation time of 20 ns (or 4ns for the un-productive orientations) and the trajectory recording interval of 20 ps (or 4.8 ps) was used in all MD simulations. During the MD, the atoms of constructed systems were set as restraints (force constant = 70), except for the residues with 4Å around the substrates, NADPH and the substrates.

1-(3-ethoxy-4-methoxyphenyl)-2-(methylsulfonyl)ethan-1-ol **2a**

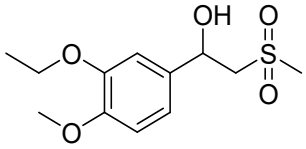

White solid, known compound[12]. $^1$H NMR (400 MHz, $CDCl_3$) δ 6.93 – 6.85 (m, 3H), 5.31 – 5.26 (m, 1H), 4.11 (q, *J* = 7.0 Hz, 2H), 3.87 (s, 3H), 3.45 (dd, *J* = 14.7, 10.2 Hz, 1H), 3.19 – 3.13 (m, 1H), 3.05 (s, 3H), 2.82 (dd, *J* = 2.7, 1.2 Hz, 1H), 1.47 (t, *J* = 7.0 Hz, 3H).

2-(methylsulfonyl)-1-phenylethan-1-ol **2b**

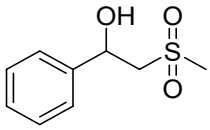

White solid, known compound[3]. $^1$H NMR (400 MHz, $CDCl_3$) δ 7.46 – 7.29 (m, 5H), 5.35 (dt, *J* = 10.2, 2.4 Hz, 1H), 3.46 (dd, *J* = 14.7, 10.2 Hz, 1H), 3.18 (d, *J* = 14.8 Hz, 1H), 3.04 (s, 3H), 2.93 (dd, *J* = 2.9, 1.1 Hz, 1H).

2-(methylsulfonyl)-1-(*p*-tolyl)ethan-1-ol **2c**

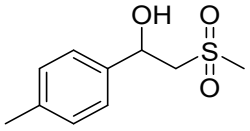

White solid, known compound[3]. $^1$H NMR (400 MHz, $CDCl_3$) δ 7.27 (d, *J* = 8.5 Hz, 2H), 7.20 (d, *J* = 8.0 Hz, 2H), 5.31 (dt, *J* = 10.2, 2.2 Hz, 1H), 3.45 (dd, *J* = 14.7, 10.2 Hz, 1H), 3.20 – 3.12 (m, 1H), 3.04 (s, 3H), 2.81 (dd, *J* = 2.7, 0.9 Hz, 1H), 2.35 (s, 3H).

1-(3-methoxyphenyl)-2-(methylsulfonyl)ethan-1-ol **2d**

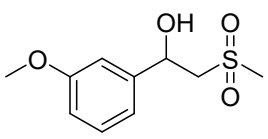

White solid. $^1$H NMR (400 MHz, $CDCl_3$) δ 7.34 – 7.26 (m, 1H), 6.98 – 6.91 (m, 2H), 6.90 – 6.83 (m, 1H), 5.32 (dt, *J* = 10.3, 2.4 Hz, 1H), 3.82 (s, 3H), 3.45 (dd, *J* = 14.8, 10.3 Hz, 1H), 3.22 – 3.13 (m, 1H), 3.05 (s, 4H), 2.93 (dd, *J* = 2.9, 1.2 Hz, 1H). $^{13}$C NMR (150 MHz, $CDCl_3$) δ 160.08, 142.76, 130.13, 117.81, 114.09, 111.22, 69.24, 62.42, 55.34, 42.88.

1-(4-methoxyphenyl)-2-(methylsulfonyl)ethan-1-ol **2e**

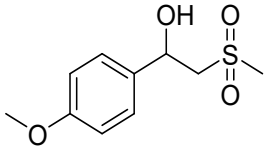


White solid, known compound[3]. $^1$H NMR (400 MHz, $CDCl_3$) δ 7.30 (d, *J* = 6.8 Hz, 2H), 6.91 (d, *J* = 8.7 Hz, 2H), 5.30 (dt, *J* = 10.2, 2.3 Hz, 1H), 3.81 (s, 3H), 3.46 (dd, *J* = 14.7, 10.2 Hz, 1H), 3.15 (ddt, *J* = 14.6, 2.2, 1.1 Hz, 1H), 3.04 (s, 3H), 2.79 (dd, *J* = 2.7, 1.0 Hz, 1H).

1-(4-fluorophenyl)-2-(methylsulfonyl)ethan-1-ol **2f**

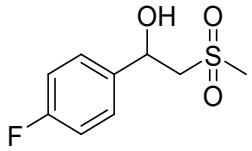


White solid. $^1$H NMR (400 MHz, $CDCl_3$) δ 7.41 – 7.34 (m, 2H), 7.13 – 7.04 (m, 2H), 5.36 (dt, *J* = 10.3, 2.4 Hz, 1H), 3.43 (dd, *J* = 14.7, 10.3 Hz, 1H), 3.21 – 3.12 (m, 1H), 3.06 (s, 3H), 2.94 (dd, *J* = 2.8, 1.0 Hz, 1H). $^{13}$C NMR (150 MHz, $CDCl_3$) δ 163.54, 161.90, 136.85 (d, *J* = 4.1 Hz), 127.48 (d, *J* = 8.0 Hz), 115.97 (d, *J* = 21.6 Hz), 68.66, 62.43, 42.88.

1-(3-chlorophenyl)-2-(methylsulfonyl)ethan-1-ol **2g**

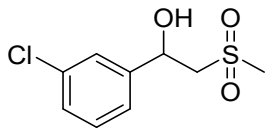


White solid. $^1$H NMR (400 MHz, $CDCl_3$) δ 7.43 – 7.41 (m, 1H), 7.36 – 7.30 (m, 2H), 7.28 – 7.24 (m, 1H), 5.35 (dd, *J* = 10.3, 1.7 Hz, 1H), 3.42 (dd, *J* = 14.7, 10.3 Hz, 1H), 3.21 – 3.14 (m, 1H), 3.07 (s, 3H). $^{13}$C NMR (150 MHz, $CDCl_3$) δ 142.98, 134.99, 130.33, 128.80, 125.91, 123.81, 68.66, 62.26, 42.93.

1-(4-chlorophenyl)-2-(methylsulfonyl)ethan-1-ol **2h**

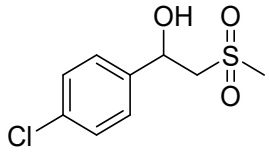


White solid, known compound[3]. $^1$H NMR (400 MHz, $CDCl_3$) δ 7.41 – 7.30 (m, 4H), 5.35 (dd, *J* = 10.3, 2.1 Hz, 1H), 3.41 (dd, *J* = 14.6, 10.3 Hz, 1H), 3.19 – 3.13 (m, 1H), 3.06 (s, 3H), 3.00 (s, 1H).

1-(4-bromophenyl)-2-(methylsulfonyl)ethan-1-ol **2i**

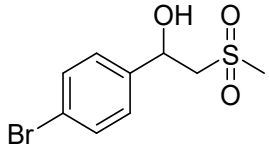


White solid. $^1$H NMR (400 MHz, $CDCl_3$) δ 7.53 (d, *J* = 8.5 Hz, 2H), 7.27 (d, *J* = 8.3 Hz, 2H), 5.34 (dt, *J* = 10.3, 2.5 Hz, 1H), 3.41 (dd, *J* = 14.6, 10.3 Hz, 1H), 3.19 – 3.12 (m, 1H), 3.06 (s, 3H), 3.00 (dd, *J* = 2.8, 0.9 Hz, 1H). $^{13}$C NMR (150 MHz, $CDCl_3$) δ 139.98, 132.16, 127.37, 122.58, 68.67, 62.23, 42.90.

1-(phenylsulfonyl)propan-2-ol **2j**

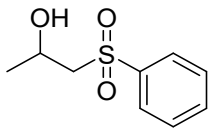


Colorless oil, known compound[5]. $^1$H NMR (400 MHz, $CDCl_3$) δ 7.97 – 7.91 (m, 2H), 7.72 – 7.66 (m, 1H), 7.64 – 7.57 (m, 2H), 4.38 – 4.29 (m, 1H), 3.40 – 3.36 (m, 1H), 3.24 (dd, *J* = 14.3, 9.0 Hz, 1H), 3.17 (dd, *J* = 14.3, 2.3 Hz, 1H), 1.25 (d, *J* = 6.4 Hz, 3H).

1-tosylpropan-2-ol **2k**

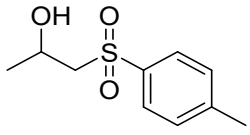

Pale yellow solid, known compound[13]. $^1$H NMR (400 MHz, $CDCl_3$) δ 7.81 (d, *J* = 8.3 Hz, 2H), 7.38 (d, *J* = 7.9 Hz, 2H), 4.31 (d, *J* = 2.2 Hz, 1H), 3.42 (s, 1H), 3.21 (dd, *J* = 14.3, 9.1 Hz, 1H), 3.14 (dd, *J* = 14.3, 2.3 Hz, 1H), 2.46 (s, 3H), 1.24 (d, *J* = 6.4 Hz, 3H).

1-phenyl-2-(phenylsulfonyl)ethan-1-ol **2l**

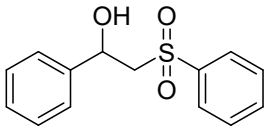


White solid, known compound[3]. $^1$H NMR (400 MHz, $CDCl_3$) δ 8.00 – 7.93 (m, 2H), 7.72 – 7.66 (m, 1H), 7.63 – 7.56 (m, 2H), 7.36 – 7.26 (m, 5H), 5.28 (dd, *J* = 10.0, 1.7 Hz, 1H), 3.78 – 3.56 (m, 1H), 3.51 (dd, *J* = 14.4, 10.1 Hz, 1H), 3.35 (dd, *J* = 14.4, 1.8 Hz, 1H).

1-(4-methoxyphenyl)-2-(phenylsulfonyl)ethan-1-ol **2m**

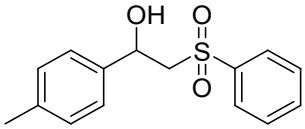


White solid, known compound[3]. $^1$H NMR (400 MHz, $CDCl_3$) δ 7.98 – 7.93 (m, 2H), 7.72 – 7.66 (m, 1H), 7.59 (t, *J* = 7.6 Hz, 2H), 7.20 – 7.10 (m, 4H), 5.24 (d, *J* = 10.0 Hz, 1H), 3.55 (d, *J* = 2.2 Hz, 1H), 3.50 (dd, *J* = 14.4, 10.0 Hz, 1H), 3.33 (dd, *J* = 14.4, 1.8 Hz, 1H), 2.31 (s, 3H).

1-(2-methoxyphenyl)-2-(phenylsulfonyl)ethan-1-ol **2n**

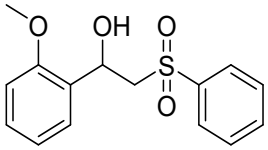


White solid, known compound[3]. $^1$H NMR (400 MHz, $CDCl_3$) δ 7.98 – 7.93 (m, 2H), 7.70 – 7.65 (m, 1H), 7.61 – 7.55 (m, 2H), 7.47 (dd, *J* = 7.6, 1.2 Hz, 1H), 7.23 (td, *J* = 8.0, 1.7 Hz, 1H), 6.96 (td, *J* = 7.5, 0.8 Hz, 1H), 6.74 (d, *J* = 8.2 Hz, 1H), 5.34 (dd, *J* = 9.3, 1.8 Hz, 1H), 3.60 (s, 3H), 3.56 (dd, *J* = 14.5, 2.0 Hz, 1H), 3.42 (dd, *J* = 14.5, 9.3 Hz, 1H).

1-(3-methoxyphenyl)-2-(phenylsulfonyl)ethan-1-ol **2o**

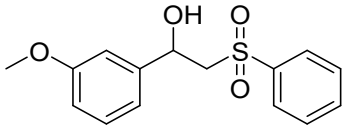

White solid, known compound[3]. $^1$H NMR (400 MHz, $CDCl_3$) δ 7.97 (d, *J* = 7.4 Hz, 2H), 7.72 – 7.66 (m, 1H), 7.60 (t, *J* = 7.8 Hz, 2H), 7.23 (t, *J* = 7.9 Hz, 1H), 6.89 – 6.79 (m, 3H), 5.26 (d, *J* = 10.0 Hz, 1H), 3.78 (s, 3H), 3.61 (s, 1H), 3.50 (dd, *J* = 14.4, 10.0 Hz, 1H), 3.35 (dd, *J* = 14.4, 1.8 Hz, 1H).

1-(4-methoxyphenyl)-2-(phenylsulfonyl)ethan-1-ol **2p**

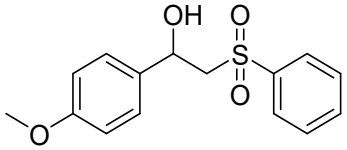

White solid, known compound[3]. $^1$H NMR (400 MHz, $CDCl_3$) δ 7.98 – 7.94 (m, 2H), 7.69 (t, *J* = 7.4 Hz, 1H), 7.59 (t, *J* = 7.6 Hz, 2H), 7.21 (d, *J* = 8.6 Hz, 2H), 6.84 (d, *J* = 8.8 Hz, 2H), 5.26 – 5.21 (m, 1H), 3.78 (s, 3H), 3.55 (d, *J* = 2.0 Hz, 1H), 3.50 (dd, *J* = 14.3, 10.0 Hz, 1H), 3.32 (dd, *J* = 14.3, 1.9 Hz, 1H).

1-(4-fluorophenyl)-2-(phenylsulfonyl)ethan-1-ol **2q**

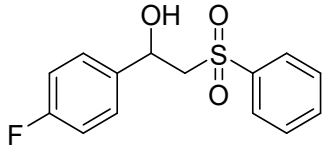

White solid, known compound[3]. $^1$H NMR (400 MHz, $CDCl_3$) δ 7.96 (dd, *J* = 8.4, 1.2 Hz, 2H), 7.73 – 7.68 (m, 1H), 7.61 (td, *J* = 7.0, 1.6 Hz, 2H), 7.31 – 7.26 (m, 2H), 7.01 (t, *J* = 8.7 Hz, 2H), 5.28 (dt, *J* = 10.0, 2.1 Hz, 1H), 3.70 (d, *J* = 2.1 Hz, 1H), 3.47 (dd, *J* = 14.3, 10.0 Hz, 1H), 3.31 (dd, *J* = 14.3, 1.9 Hz, 1H).

1-(3-chlorophenyl)-2-(phenylsulfonyl)ethan-1-ol **2r**

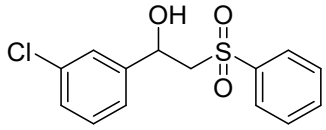

White solid, known compound[14]. $^1$H NMR (400 MHz, $CDCl_3$) δ 7.96 (dd, *J* = 8.4, 1.2 Hz, 2H), 7.73 – 7.68 (m, 1H), 7.64 – 7.58 (m, 2H), 7.32 (s, 1H), 7.25 (d, *J* = 1.2 Hz, 2H), 7.20 – 7.16 (m, 1H), 5.27 (d, *J* = 10.0 Hz, 1H), 3.75 (d, *J* = 2.1 Hz, 1H), 3.46 (dd, *J* = 14.3, 10.0 Hz, 1H), 3.33 (dd, *J* = 14.3, 1.9 Hz, 1H).

1-(4-chlorophenyl)-2-(phenylsulfonyl)ethan-1-ol **2s**

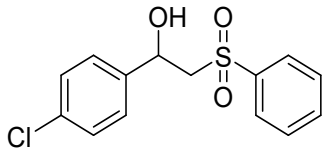


White solid, known compound[3]. $^1$H NMR (400 MHz, $CDCl_3$) δ 7.96 (dd, *J* = 8.4, 1.2 Hz, 2H), 7.73 – 7.68 (m, 1H), 7.64 – 7.58 (m, 2H), 7.32 – 7.28 (m, 2H), 7.26 – 7.22 (m, 2H), 5.28 (dt, *J* = 10.0, 2.1 Hz, 1H), 3.72 (d, *J* = 2.1 Hz, 1H), 3.45 (dd, *J* = 14.3, 10.0 Hz, 1H), 3.31 (dd, *J* = 14.3, 1.9 Hz, 1H).

1-(4-bromophenyl)-2-(phenylsulfonyl)ethan-1-ol **2t**

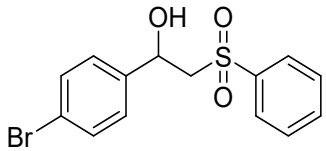


White solid, known compound[3]. $^1$H NMR (400 MHz, $CDCl_3$) δ 7.96 (dd, *J* = 8.4, 1.2 Hz, 2H), 7.73 – 7.68 (m, 1H), 7.61 (t, *J* = 7.6 Hz, 2H), 7.45 (d, *J* = 8.5 Hz, 2H), 7.18 (d, *J* = 8.3 Hz, 2H), 5.26 (d, *J* = 10.0 Hz, 1H), 3.72 (d, *J* = 2.1 Hz, 1H), 3.45 (dd, *J* = 14.3, 10.0 Hz, 1H), 3.31 (dd, *J* = 14.3, 1.9 Hz, 1H).

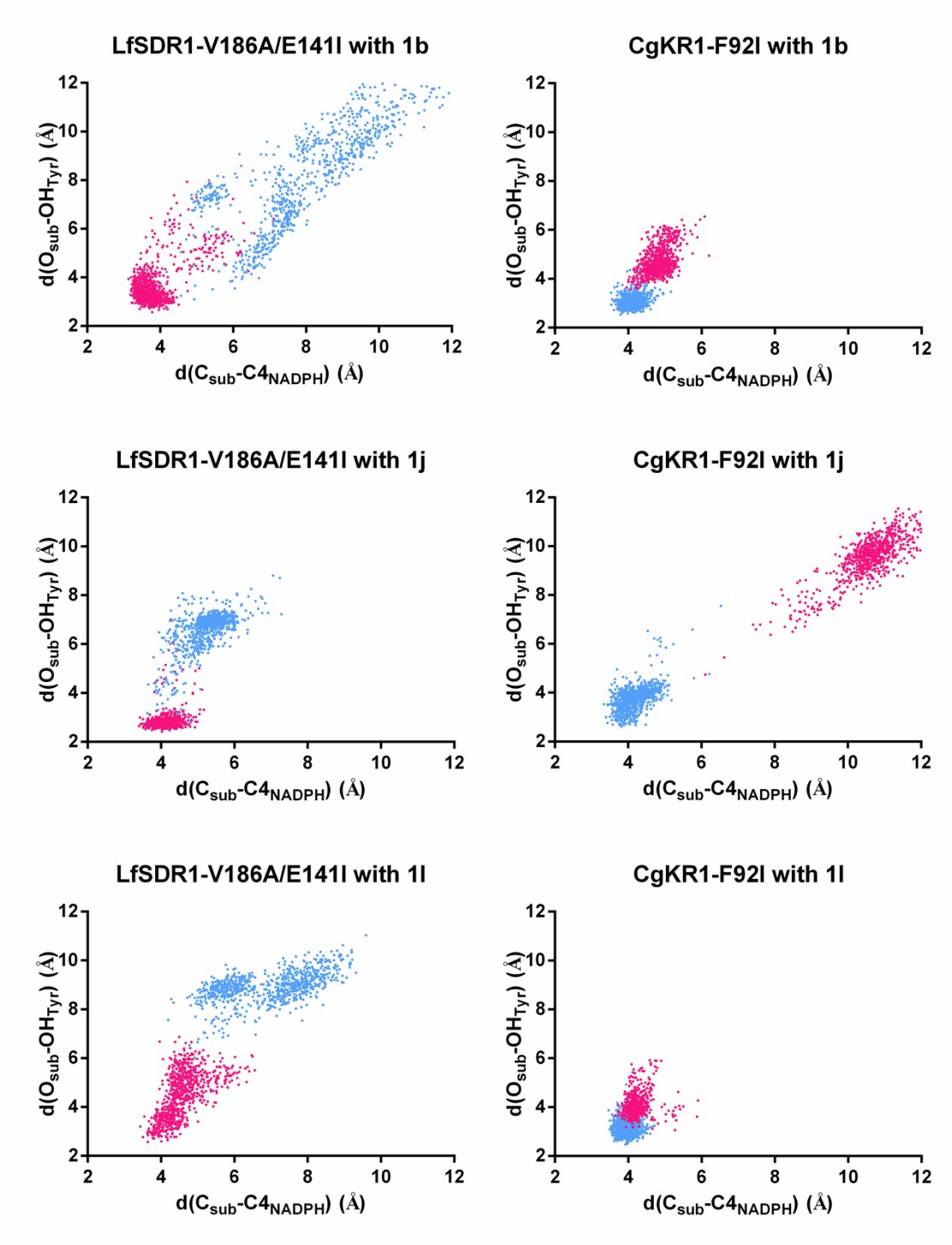


**Figure S1.** The distances of hydride transfer (NADPH-C4/carbonyl carbon of substrates) and proton donor (Tyr175-OH/carbonyl oxygen) in enzyme-substrate complexes with the pro-*R* (pink) and pro-*S* (blue) orientations.

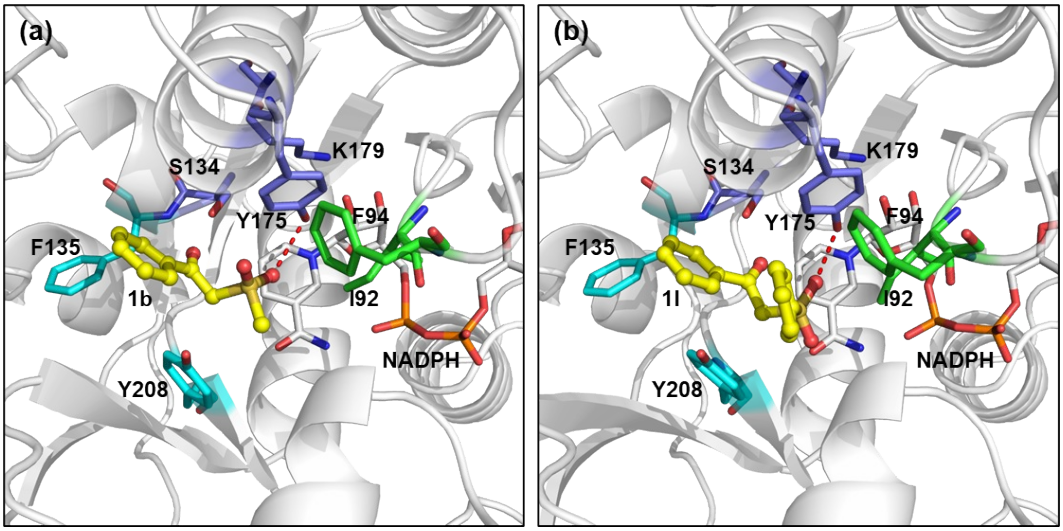


**Figure S2.** The ineffective pro-*R* models of the CgKR1-F92I with **1b** (a) and **1l** (b). The substrates are shown as yellow sticks and spheres. The catalytic residues (Ser-Tyr-Lys) and NADPH are shown as slate blue and white sticks respectively. Residues that create the left binding pocket (pocket A) are shown as cyan sticks, while residues that create the right binding pocket (pocket B) are shown as green sticks.

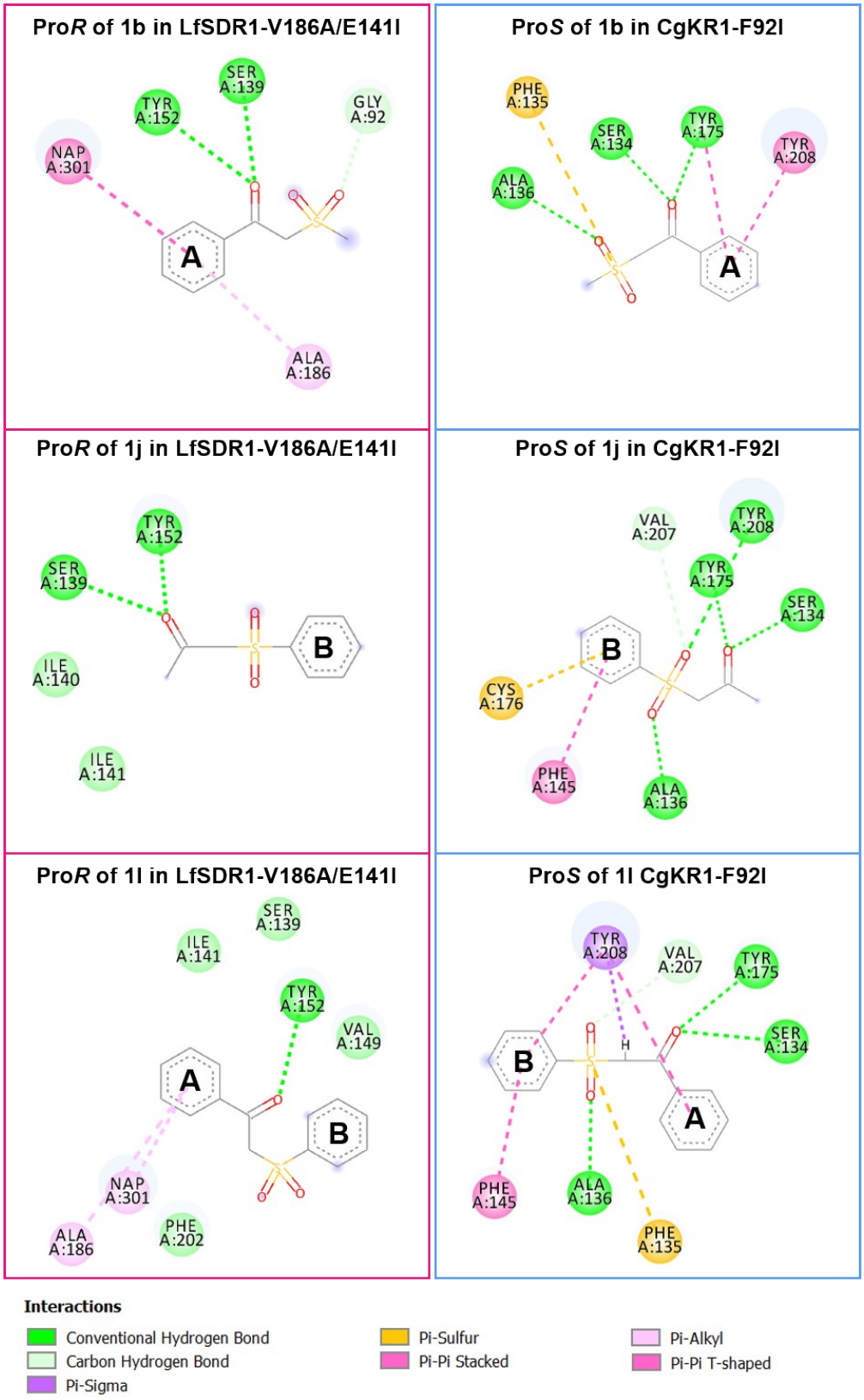


**Figure S3.** The interactions between enzyme (LfSDR1-V186A/E141I and CgKR1-F92I) and related substrates (**1b**, **1j** and **1l**). The interactions were analyzed and visualized by Discovery Studio Visualizer.

**HPLC analyses for chiral products**

1-(3-ethoxy-4-methoxyphenyl)-2-(methylsulfonyl)ethan-1-ol **2a** (HPLC: Chiracel AD-H column, 220 nm, n-hexane: i-PrOH = 80:20; flow 0.8 mL/min; $t_R$ (*R*) = 9.7 min, $t_R$ (*S*) =10.2 min).

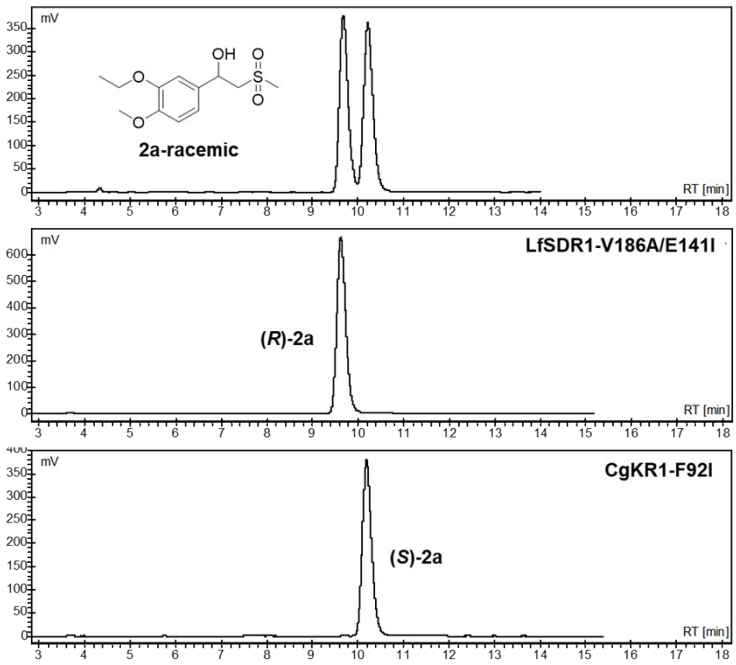


**Figure S4.** HPLC traces for the product of **2a** by KREDs catalyzed reactions.

2-(methylsulfonyl)-1-phenylethan-1-ol **2b** (HPLC: Chiracel AD-H column, 210 nm, *n*-hexane: *i*-PrOH = 90:10; flow 0.8 mL/min; $t_R$ (*R*) = 17.3 min, $t_R$ (*S*) =15.3 min).

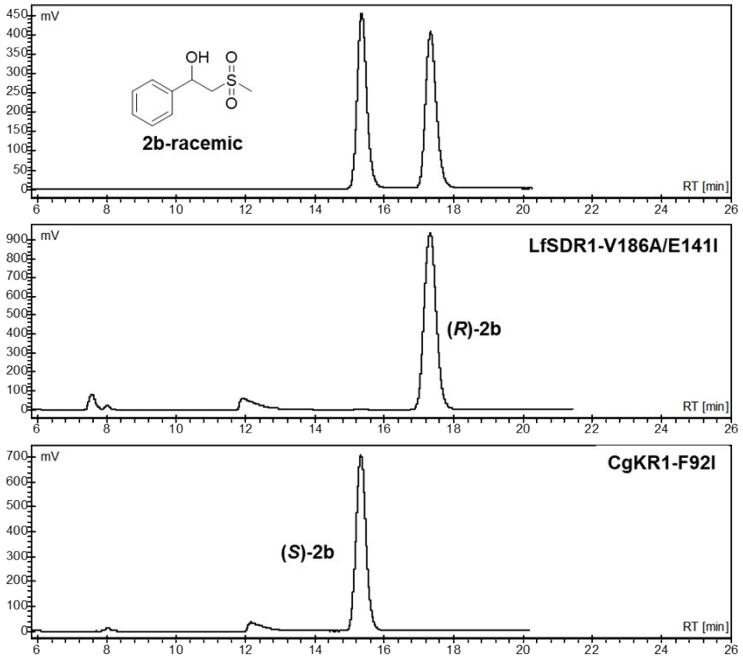


**Figure S5.** HPLC traces for the product of **2b** by KREDs catalyzed reactions.

2-(methylsulfonyl)-1-(*p*-tolyl)ethan-1-ol **2c (**HPLC: Chiracel OD-H column, 220 nm, *n*-hexane: *i*-PrOH = 80:20; flow 0.8 mL/min; $t_R$ (*R*) = 15.5 min, $t_R$ (*S*) =13.5 min).

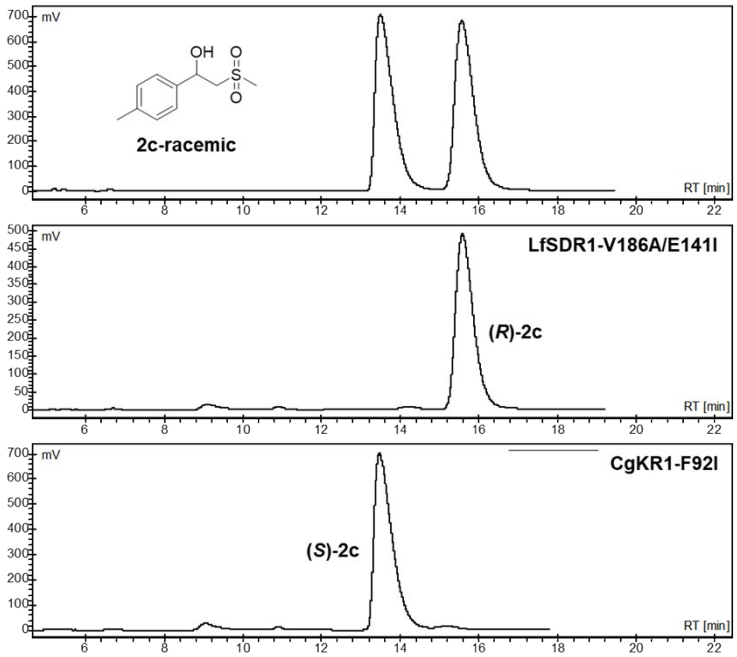


**Figure S6.** HPLC traces for the product of **2c** by KREDs catalyzed reactions.

1-(3-methoxyphenyl)-2-(methylsulfonyl)ethan-1-ol **2d** (HPLC: Chiracel AD-H column, 220 nm, *n*-hexane: *i*-PrOH = 60:40; flow 0.6 mL/min; $t_R$ (*R*) = 8.7 min, $t_R$ (*S*) =7.8 min).

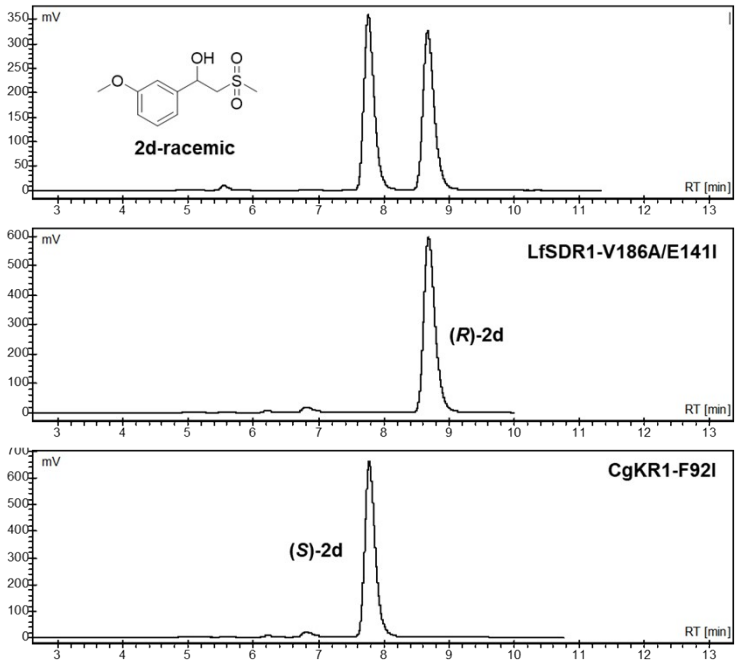


**Figure S7.** HPLC traces for the product of **2d** by KREDs catalyzed reactions.

1-(4-methoxyphenyl)-2-(methylsulfonyl)ethan-1-ol **2e (**HPLC: Chiracel OJ-H column, 220 nm, *n*-hexane: *i*-PrOH = 60:40; flow 0.6 mL/min; $t_R$ (*R*) = 33.3 min, $t_R$ (*S*) =25.1 min).

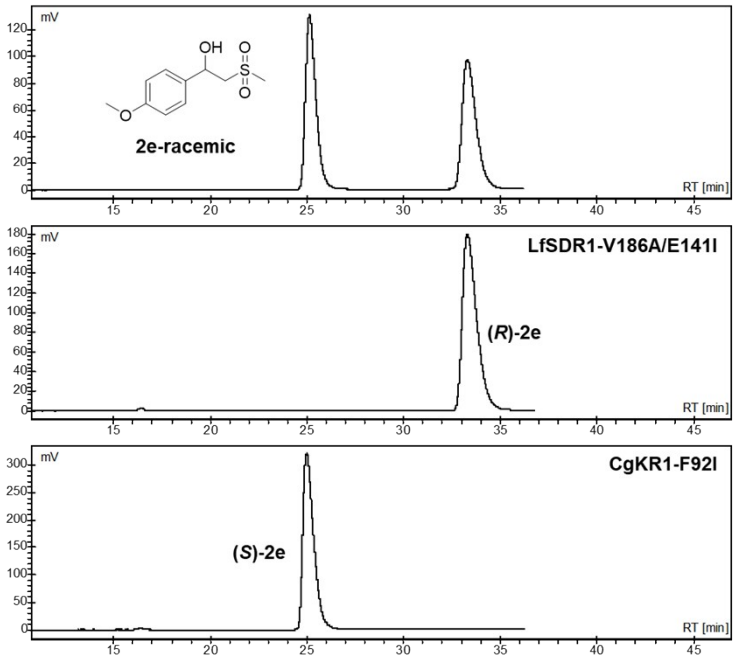


**Figure S8.** HPLC traces for the product of **2e** by KREDs catalyzed reactions.

1-(4-fluorophenyl)-2-(methylsulfonyl)ethan-1-ol **2f** (HPLC: Chiracel AD-H column, 220 nm, *n*-hexane: *i*-PrOH = 90:10; flow 0.8 mL/min; $t_R$ (*R*) = 15.5 min, $t_R$ (*S*) =16.0 min).

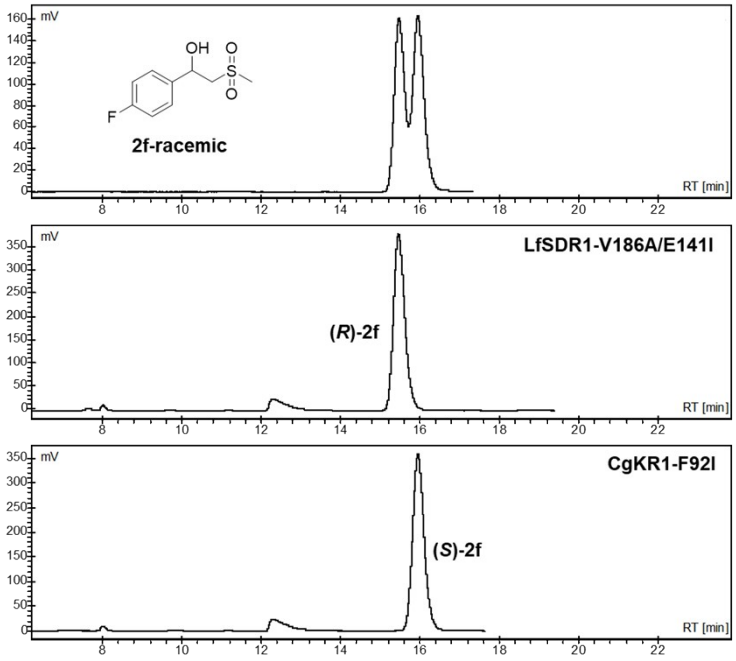


**Figure S9.** HPLC traces for the product of **2f** by KREDs catalyzed reactions.

1-(3-chlorophenyl)-2-(methylsulfonyl)ethan-1-ol **2g** (HPLC: Chiracel AD-H column, 220 nm, *n*-hexane: *i*-PrOH = 90:10; flow 0.8 mL/min; $t_R$ (*R*) = 14.9 min, $t_R$ (*S*) = 12.4 min).

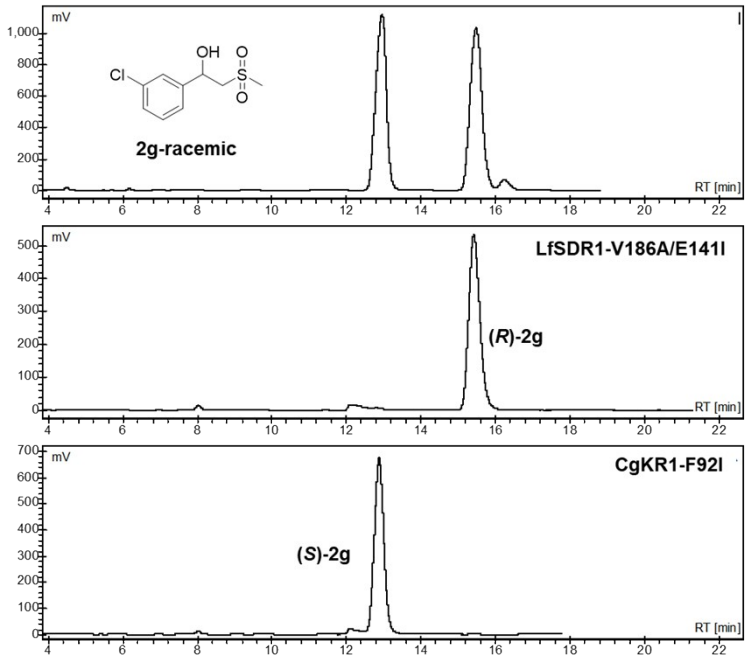


**Figure S10.** HPLC traces for the product of **2g** by KREDs catalyzed reactions.

1-(4-chlorophenyl)-2-(methylsulfonyl)ethan-1-ol **2h** (HPLC :Chiracel AD-H column, 220 nm, *n*-hexane: *i*-PrOH = 90:10; flow 0.8 mL/min; $t_R$ (*R*) = 16.4 min, $t_R$ (*S*) = 17.1 min).

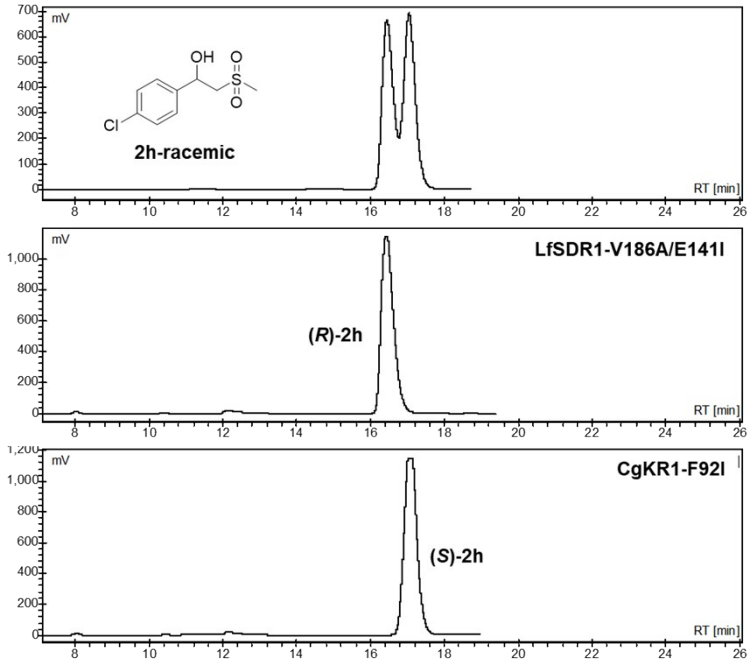


**Figure S11.** HPLC traces for the product of **2h** by KREDs catalyzed reactions.

1-(4-bromophenyl)-2-(methylsulfonyl)ethan-1-ol **2i** (HPLC: Chiracel OJ-H column, 220 nm, *n*-hexane: *i*-PrOH = 60:40; flow 0.6 mL/min; $t_R$ (*R*) = 23.2 min, $t_R$ (*S*) = 21.8 min).

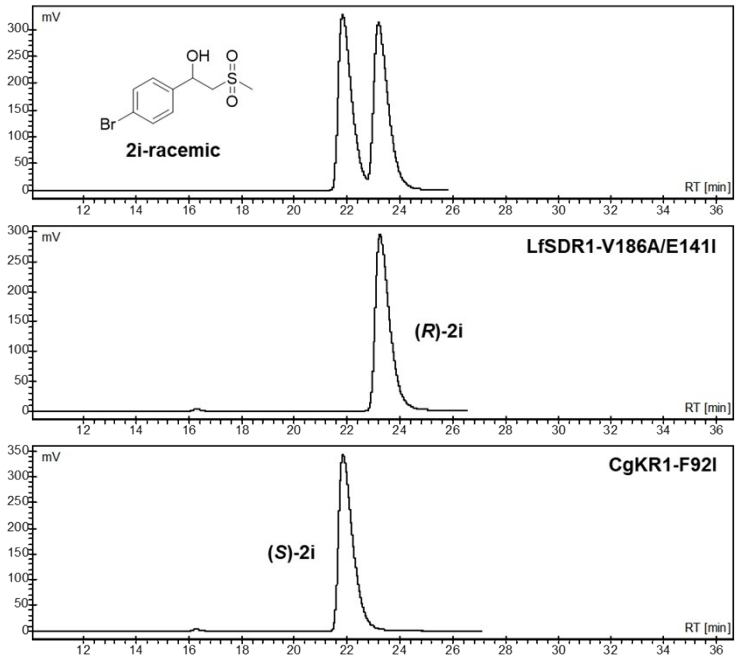


**Figure S12.** HPLC traces for the product of **2i** by KREDs catalyzed reactions.

1-(phenylsulfonyl)propan-2-ol **2j** (HPLC: Chiracel AD-H column, 220 nm, *n*-hexane: *i*-PrOH = 70:30; flow 0.8 mL/min; $t_R$ (*R*) = 18.3 min, $t_R$ (*S*) = 11.2 min).

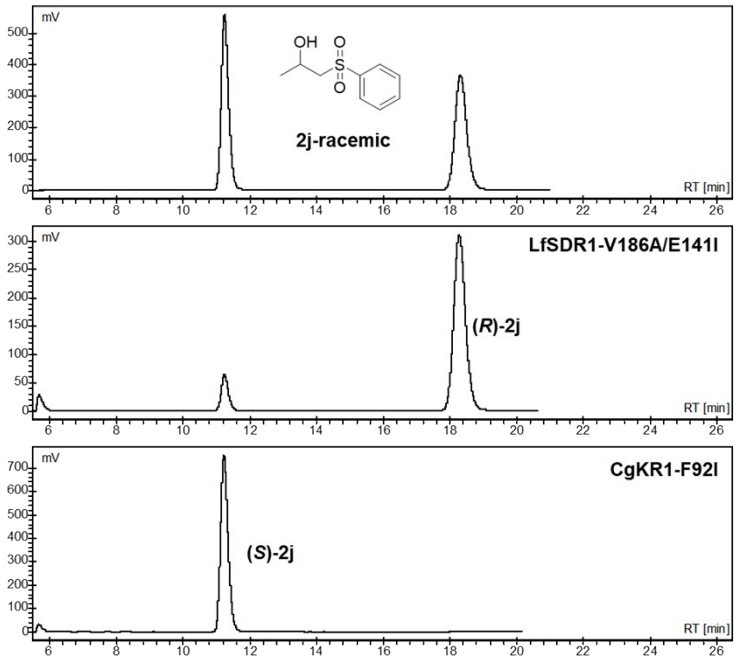


**Figure S13.** HPLC traces for the product of **2j** by KREDs catalyzed reactions.

1-tosylpropan-2-ol **2k** (HPLC: Chiracel AD-H column, 220 nm, *n*-hexane: *i*-PrOH = 90:10; flow 0.8 mL/min; $t_R$ (*R*) = 37.3 min, $t_R$ (*S*) = 33.8 min).

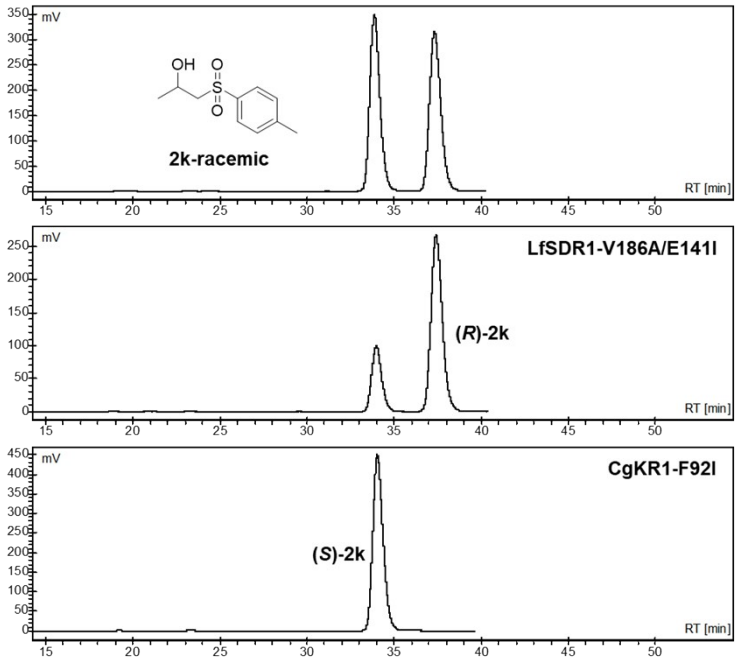


**Figure S14.** HPLC traces for the product of **2k** by KREDs catalyzed reactions.

1-phenyl-2-(phenylsulfonyl)ethan-1-ol **2l** (HPLC: Chiracel AD-H column, 220 nm, *n*-hexane: *i*-PrOH = 70:30; flow 0.8 mL/min; $t_R$ (*R*) = 11.9 min, $t_R$ (*S*) = 13.6 min.

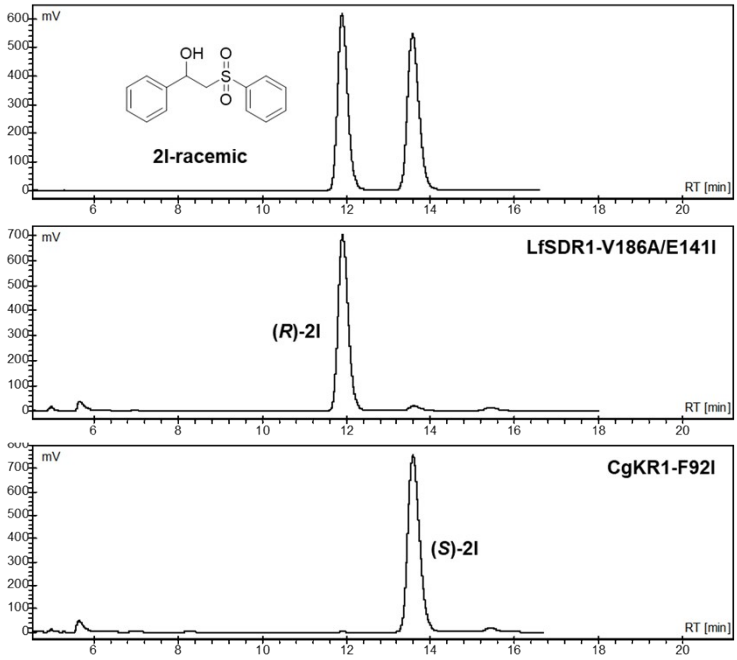


**Figure S15.** HPLC traces for the product of **2l** by KREDs catalyzed reactions.

1-(4-methoxyphenyl)-2-(phenylsulfonyl)ethan-1-ol **2m** (HPLC: AD-H column, 220 nm, *n*-hexane: *i*-PrOH = 60:40; flow 0.6 mL/min; $t_R$ (*R*) = 14.3 min, $t_R$ (*S*) = 15.3 min).

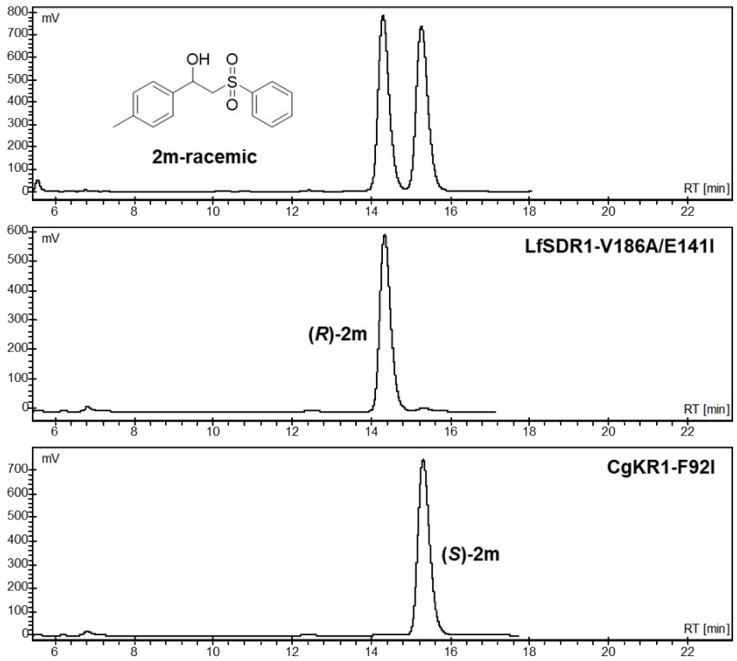


**Figure S16.** HPLC traces for the product of **2m** by KREDs catalyzed reactions.

1-(2-methoxyphenyl)-2-(phenylsulfonyl)ethan-1-ol **2n** (HPLC: Chiracel AD-H column, 210 nm, *n*-hexane: *i*-PrOH = 80:20; flow 0.8 mL/min; $t_R$ (*R*) = 18.4 min, $t_R$ (*S*) = 21.7 min).

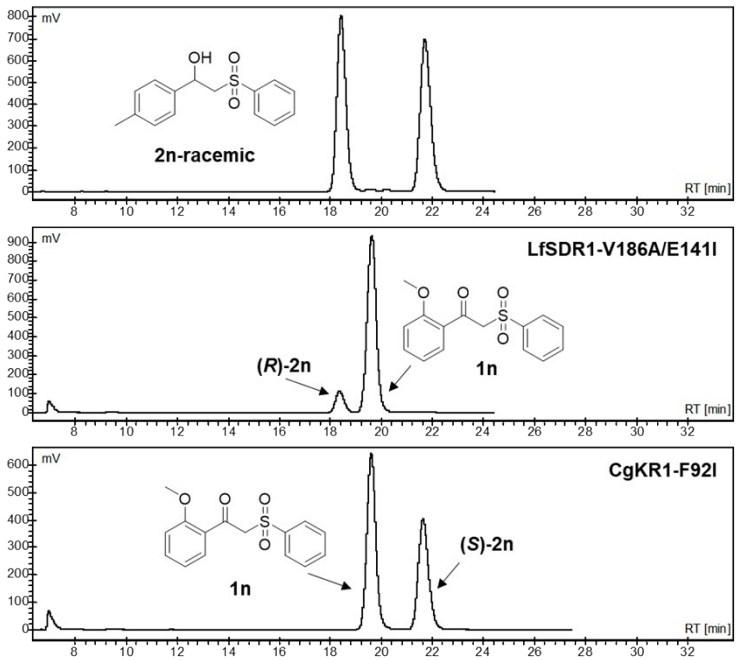


**Figure S17.** HPLC traces for the product of **2n** by KREDs catalyzed reactions.

1-(3-methoxyphenyl)-2-(phenylsulfonyl)ethan-1-ol **2o** (HPLC: Chiracel AD-H column, 220 nm, *n*-hexane: *i*-PrOH = 60:40; flow 0.6 mL/min; $t_R$ (*R*) = 14.5 min, $t_R$ (*S*) = 15.3 min).

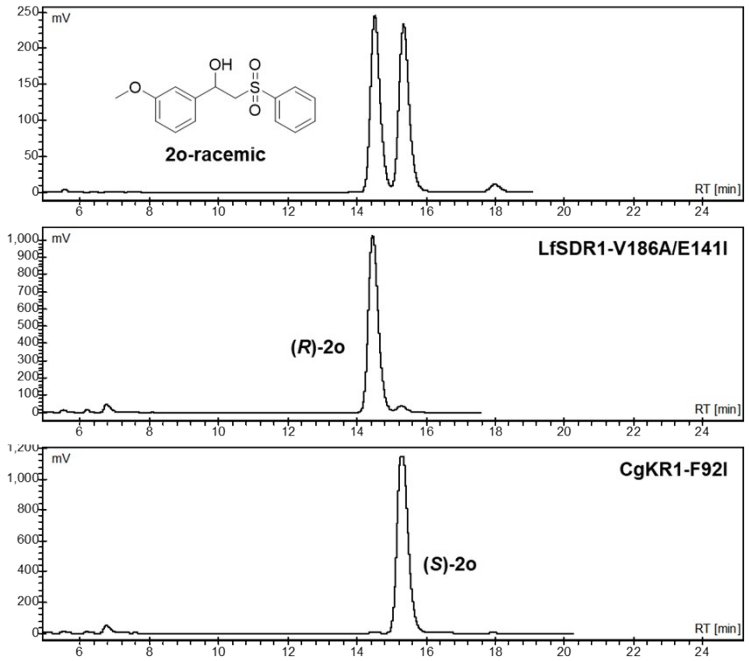


**Figure S18.** HPLC traces for the product of **2o** by KREDs catalyzed reactions.

1-(4-methoxyphenyl)-2-(phenylsulfonyl)ethan-1-ol **2p** (HPLC: Chiracel OJ-H column, 220 nm, *n*-hexane: *i*-PrOH = 60:40; flow 0.6 mL/min; $t_R$ (*R*) = 30.8 min, $t_R$ (*S*) = 43.4 min).

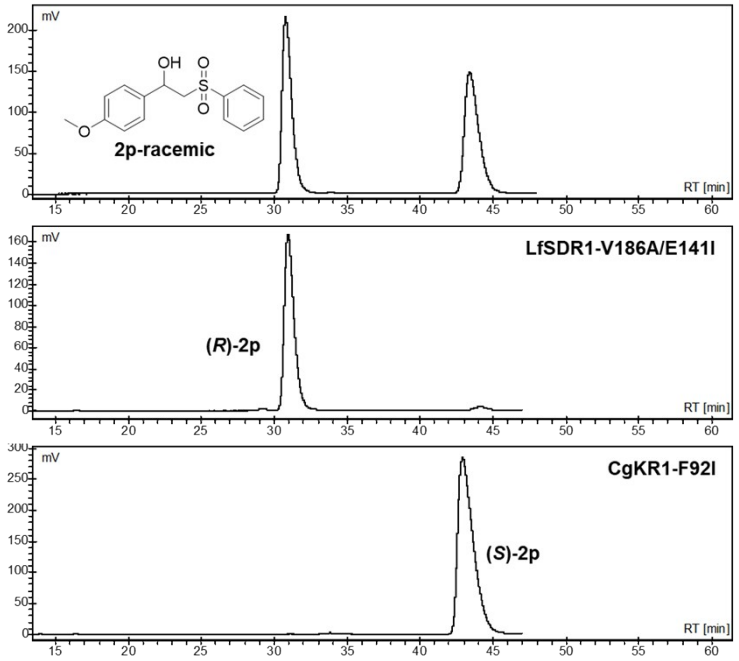


**Figure S19.** HPLC traces for the product of **2p** by KREDs catalyzed reactions.

1-(4-fluorophenyl)-2-(phenylsulfonyl)ethan-1-ol **2q** (HPLC on Chiracel AD-H column, 220 nm, *n*-hexane: *i*-PrOH = 60:40; flow 0.6 mL/min; $t_R$ (*R*) = 13.5 min, $t_R$ (*S*) = 14.8 min).

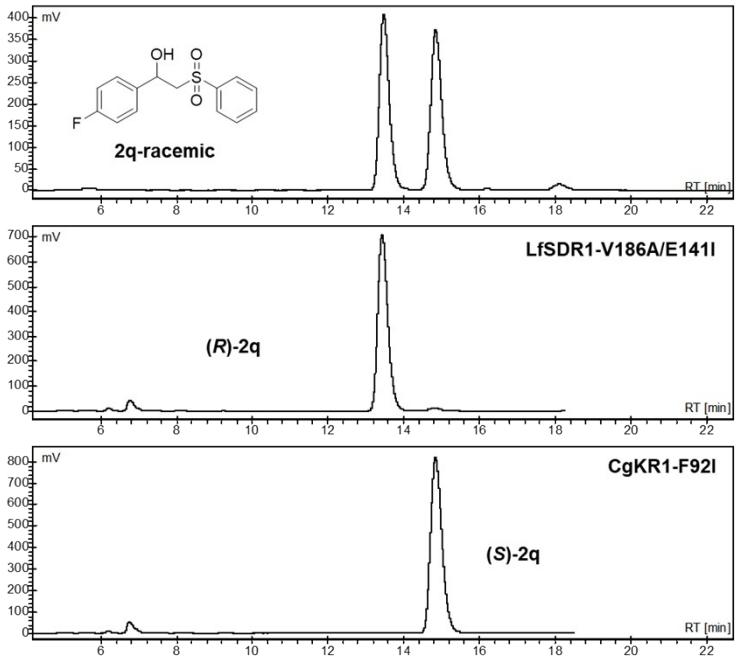


**Figure S20.** HPLC traces for the product of **2q** by KREDs catalyzed reactions.

1-(3-chlorophenyl)-2-(phenylsulfonyl)ethan-1-ol **2r** (HPLC: Chiracel AD-H column, 220 nm, *n*-hexane: *i*-PrOH = 80:20; flow 0.8 mL/min; $t_R$ (*R*) = 14.5 min, $t_R$ (*S*) = 17.3 min).

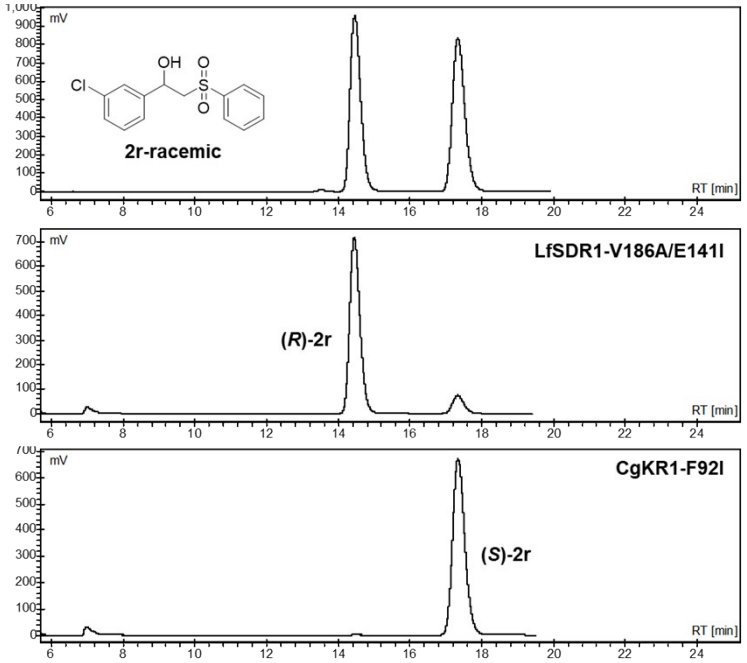


**Figure S21.** HPLC traces for the product of **2r** by KREDs catalyzed reactions.

1-(4-chlorophenyl)-2-(phenylsulfonyl)ethan-1-ol **2s** (HPLC: Chiracel AD-H column, 220 nm, *n*-hexane: *i*-PrOH = 60:40; flow 0.6 mL/min; $t_R$ (*R*) = 15.0 min, $t_R$ (*S*) = 15.9 min).

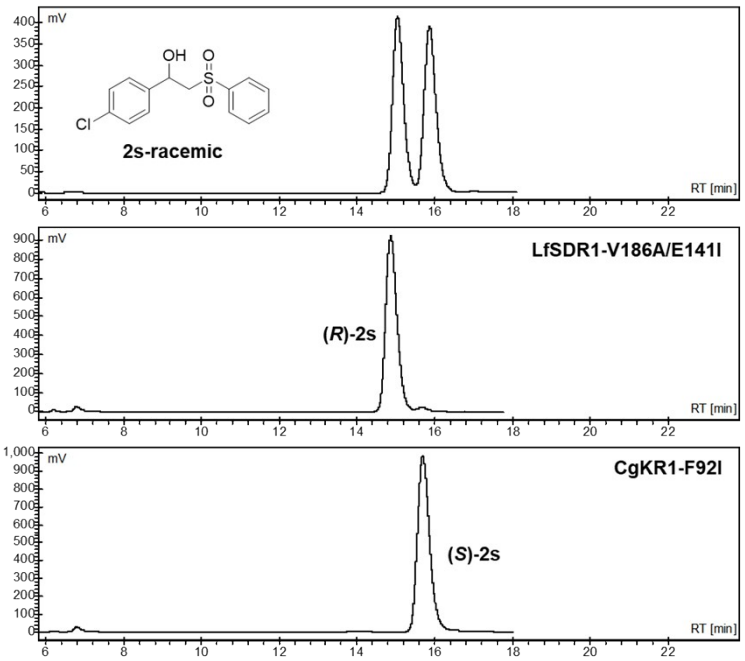


**Figure S22.** HPLC traces for the product of **2s** by KREDs catalyzed reactions.

1-(4-bromophenyl)-2-(phenylsulfonyl)ethan-1-ol **2t** (HPLC: Chiracel OJ-H column, 220 nm, *n*-hexane: *i*-PrOH = 60:40; flow 0.6 mL/min; $t_R$ (*R*) = 25.1 min, $t_R$ (*S*) = 32.6 min).

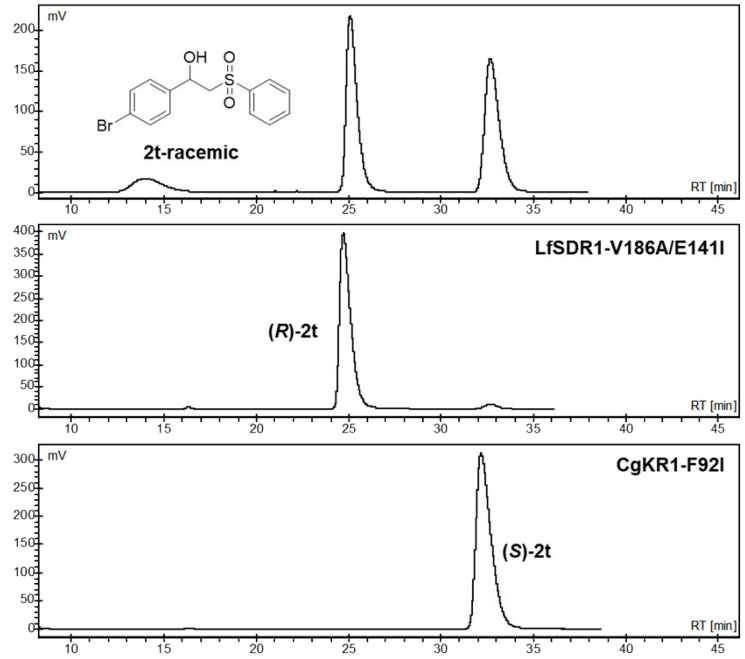


**Figure S23.** HPLC traces for the product of **2t** by KREDs catalyzed reactions.

## NMR spectra

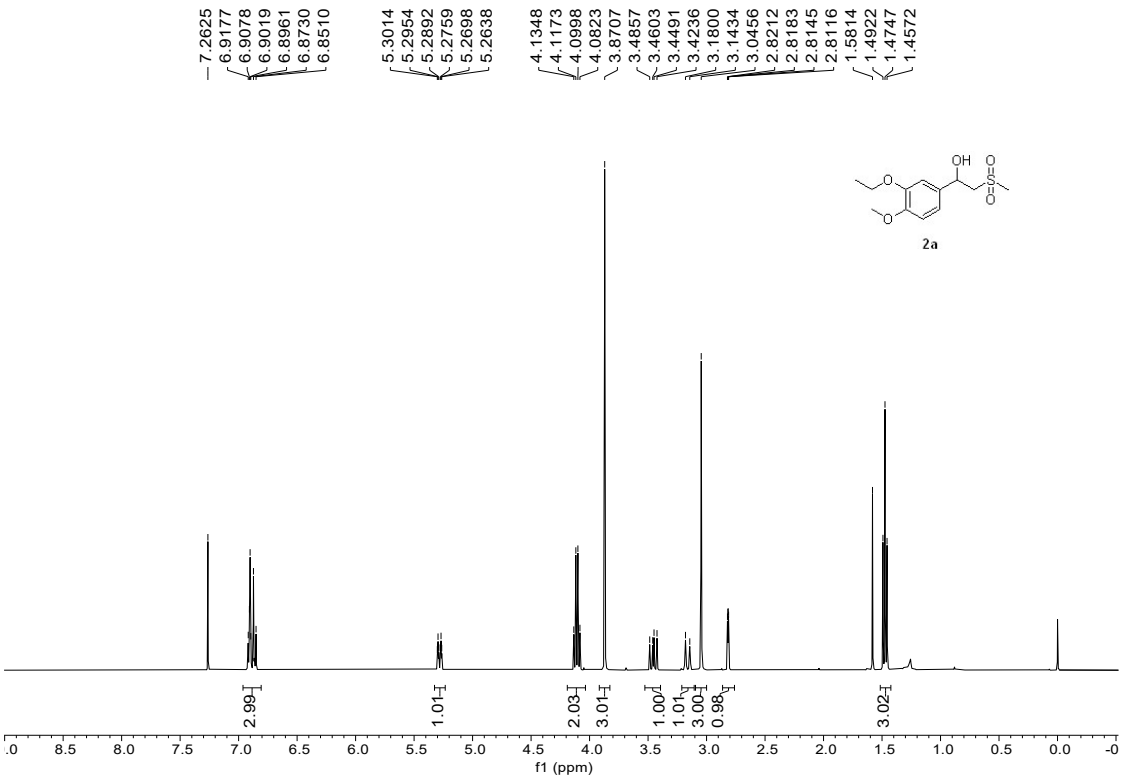


**Figure S24.** $^{1}$H NMR spectrum of **2a** (400 MHz, in $CDCl_3$).

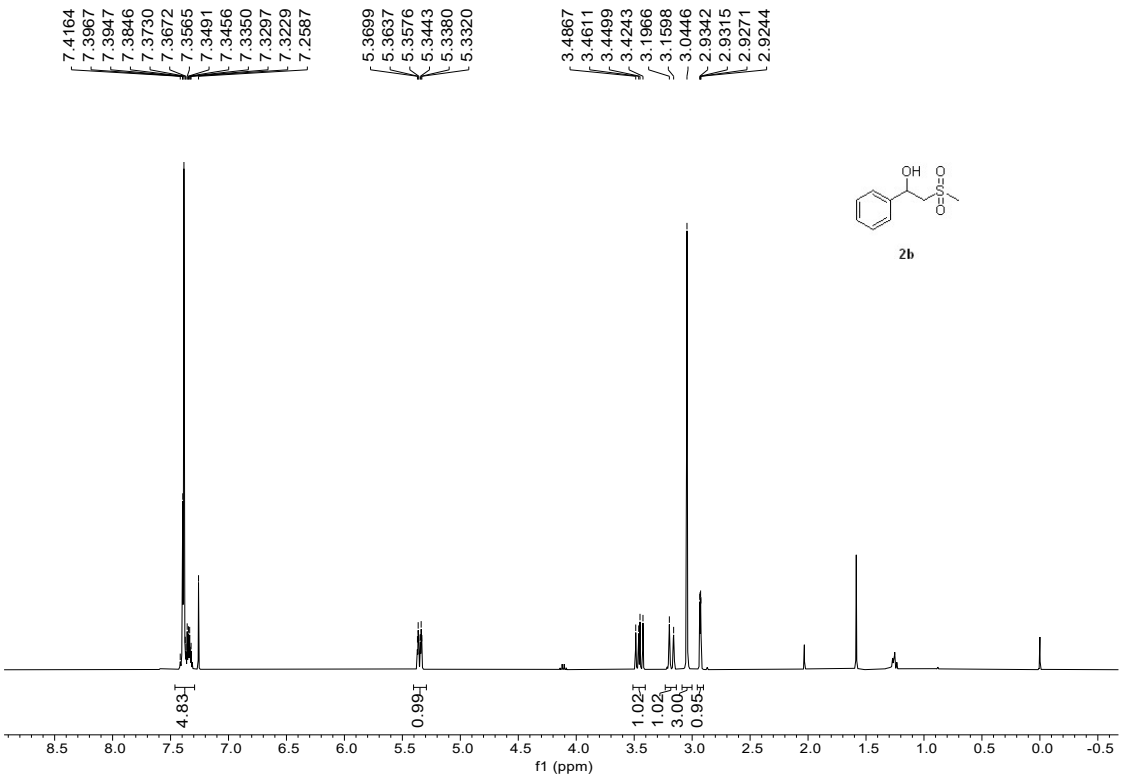


**Figure S25.** $^{1}$H NMR spectrum of **2b** (400 MHz, in $CDCl_3$).

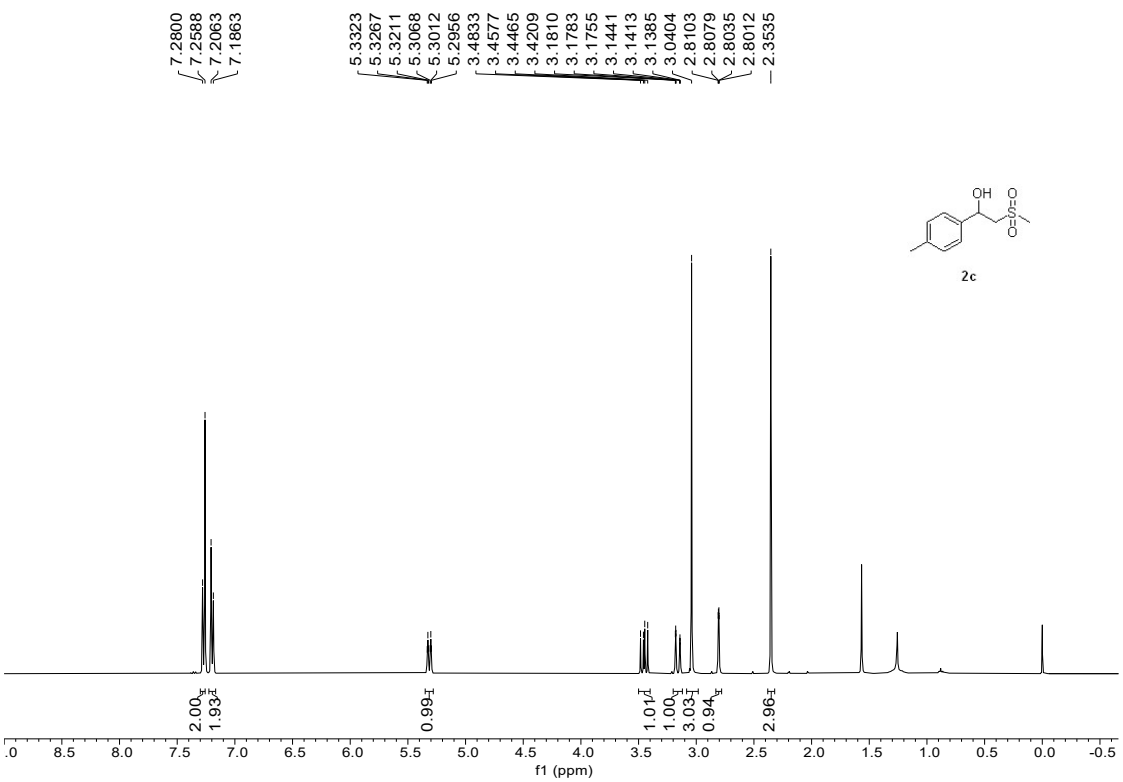

**Figure S26.** $^1$H NMR spectrum of **2c** (400 MHz, in $CDCl_3$).

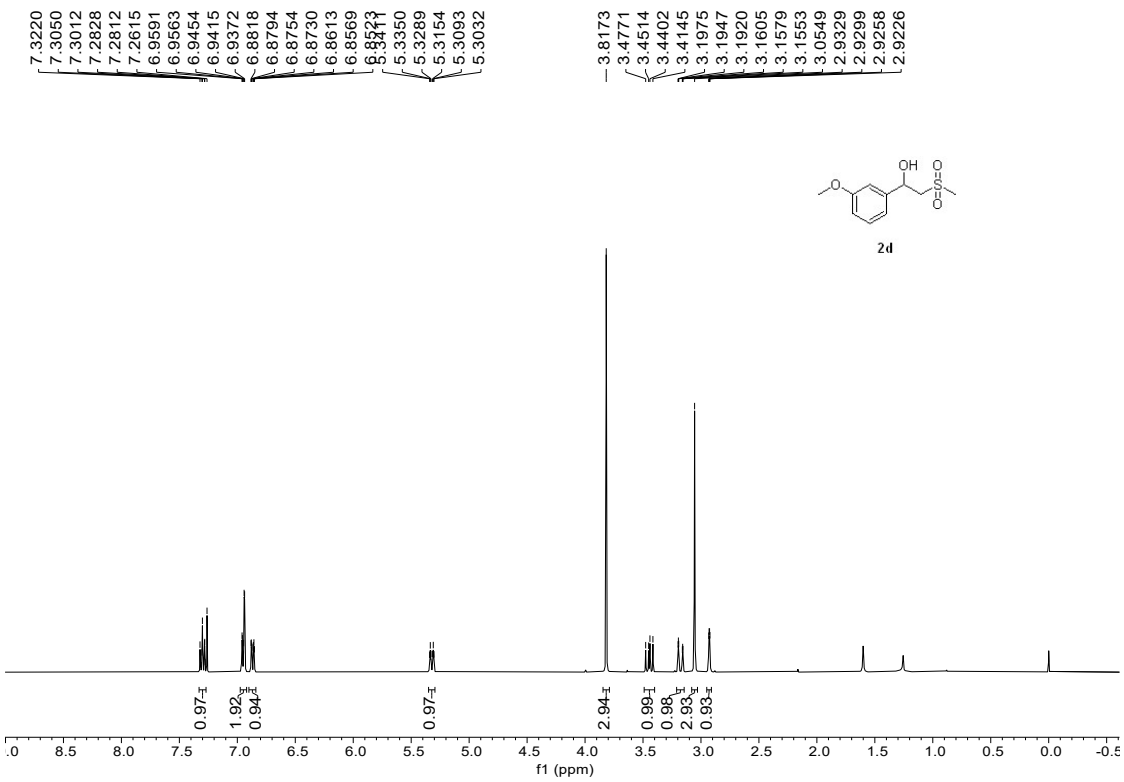


**Figure S27.** $^1$H NMR spectrum of **2d** (400 MHz, in $CDCl_3$).

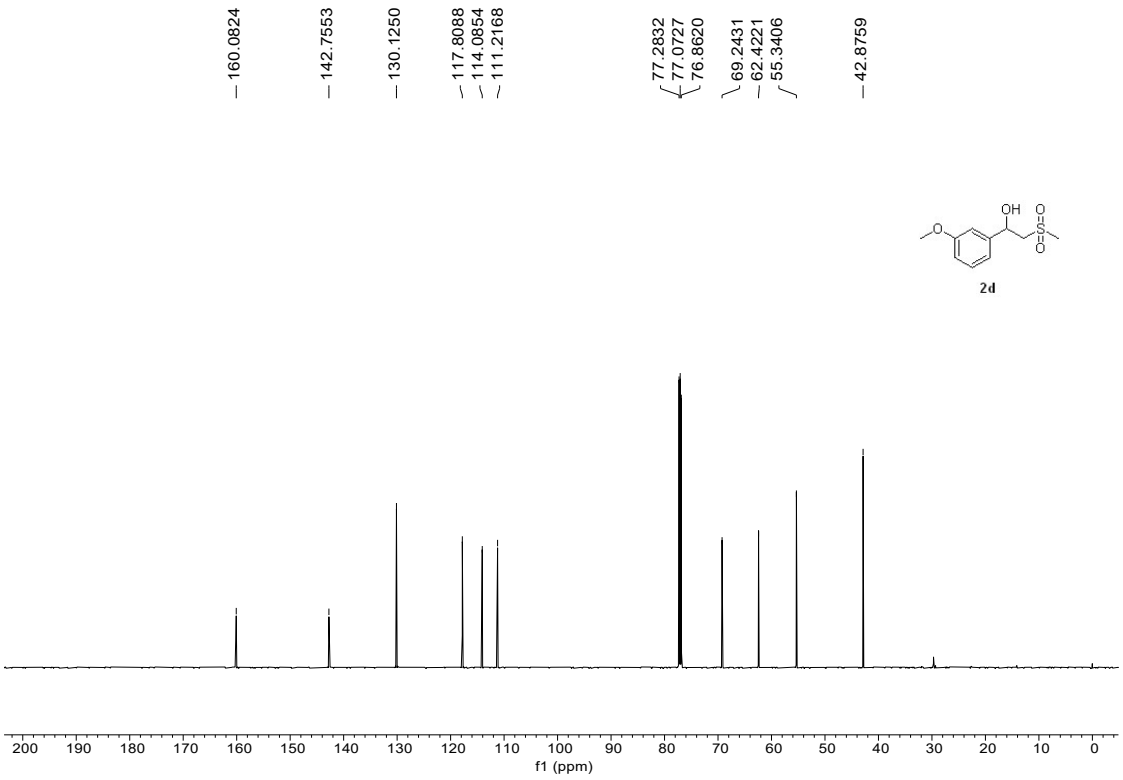


**Figure S28.** $^{13}C$ NMR spectrum of **2d** (150 MHz, in $CDCl_3$).

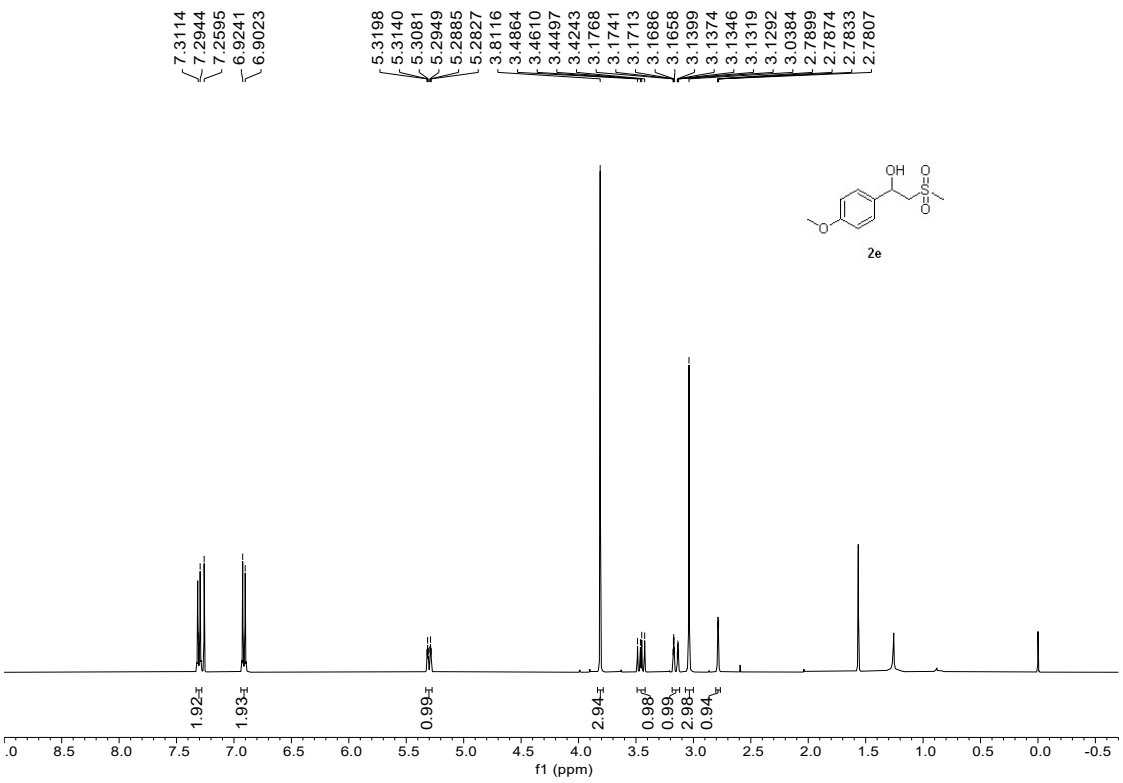


**Figure S29.** $^{1}H$ NMR spectrum of **2e** (400 MHz, in $CDCl_3$).

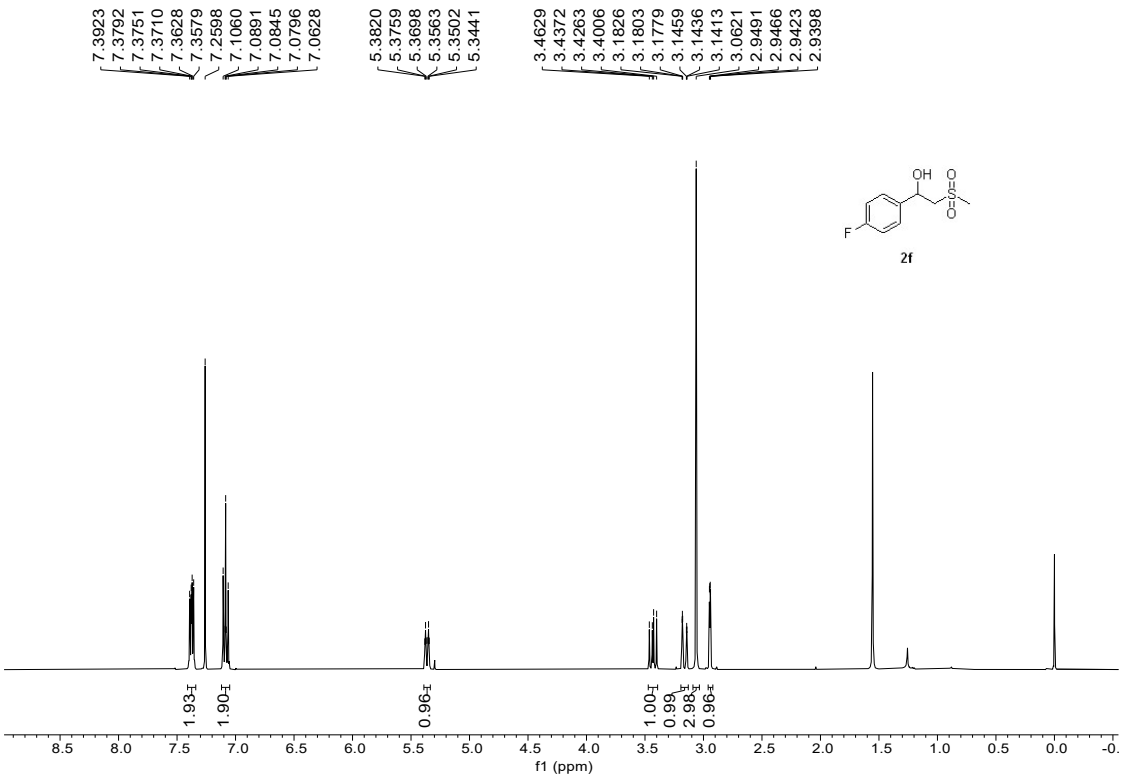


**Figure S30.** $^{1}$H NMR spectrum of **2f** (400 MHz, in $CDCl_3$).

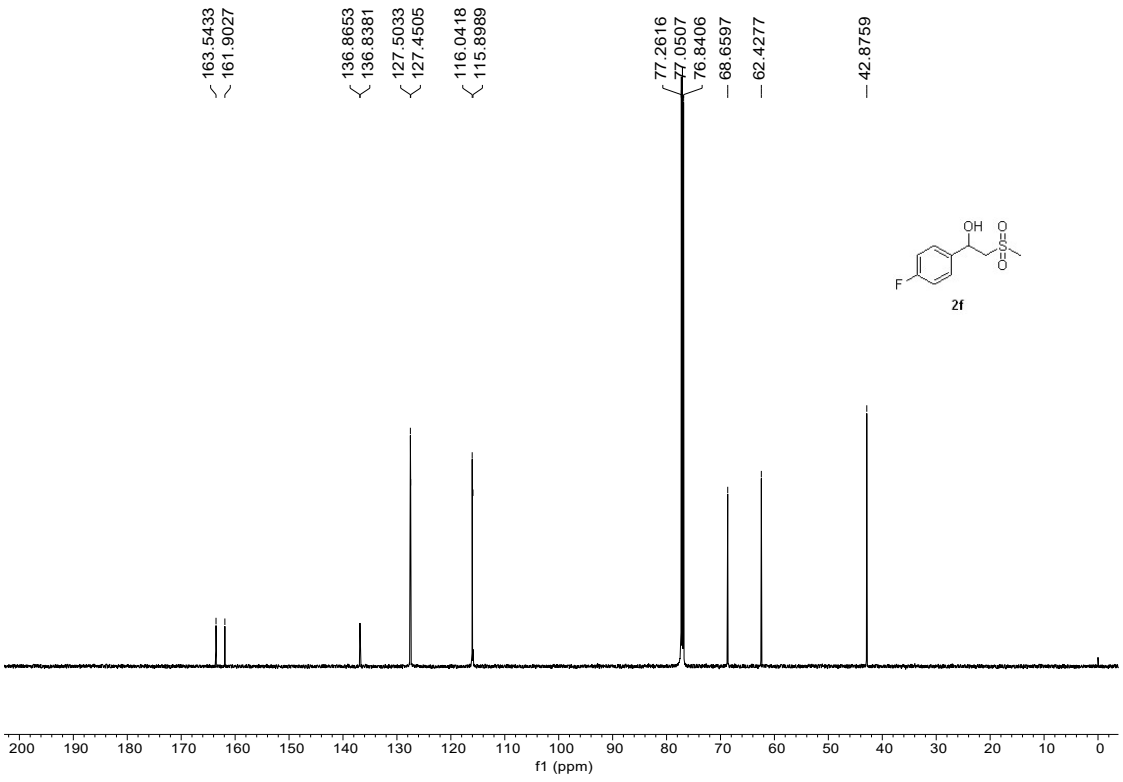


**Figure S31.** $^{13}$C NMR spectrum of **2f** (150 MHz, in $CDCl_3$).

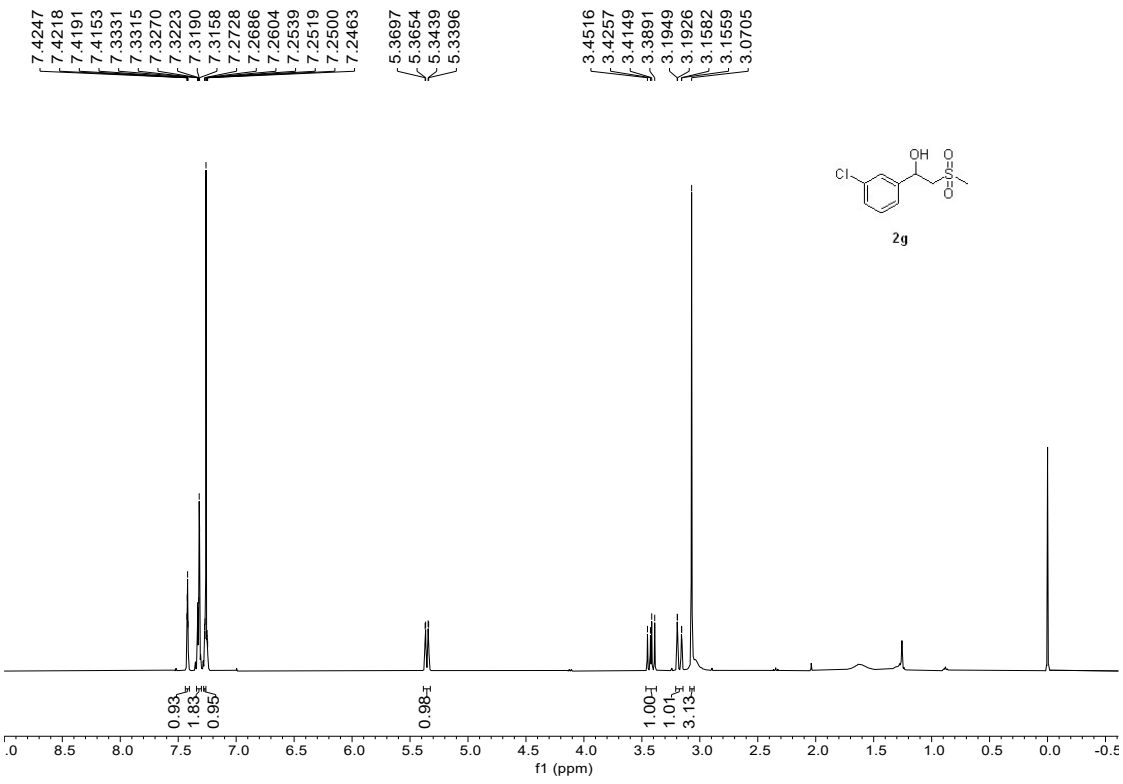


**Figure S32.** $^{1}$H NMR spectrum of **2g** (400 MHz, in $CDCl_3$).

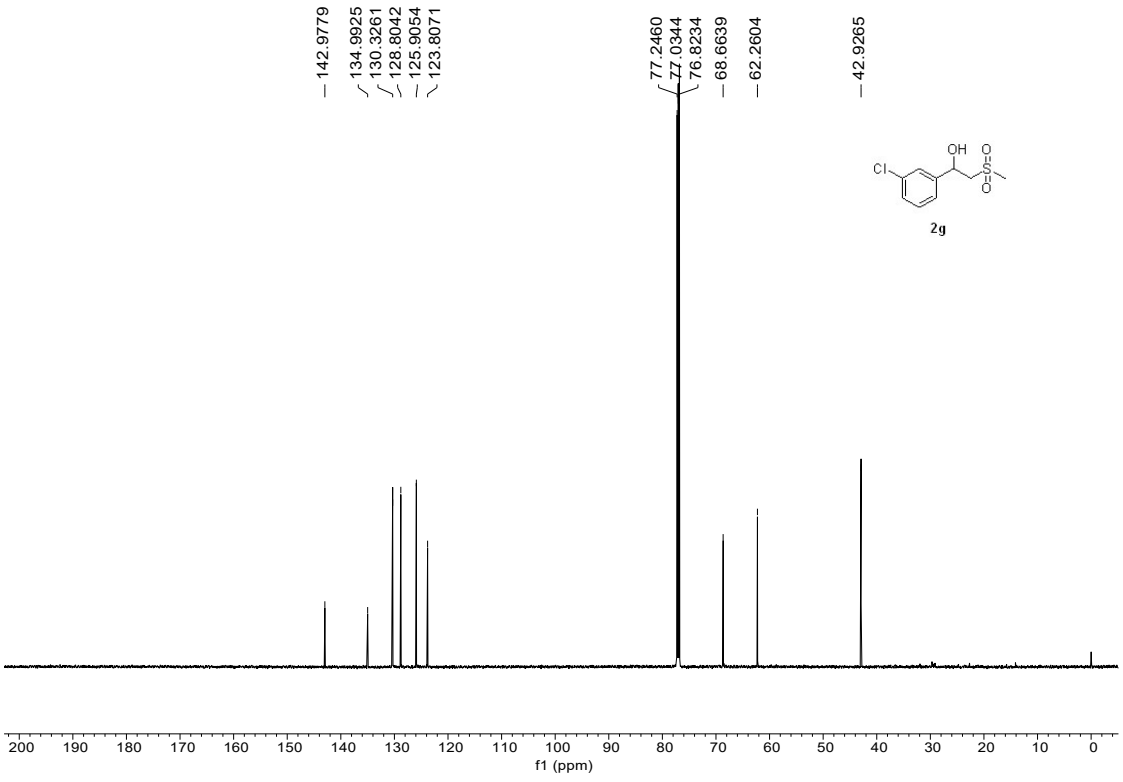

**Figure S33.** $^{13}C$ NMR spectrum of **2g** (150 MHz, in $CDCl_3$).

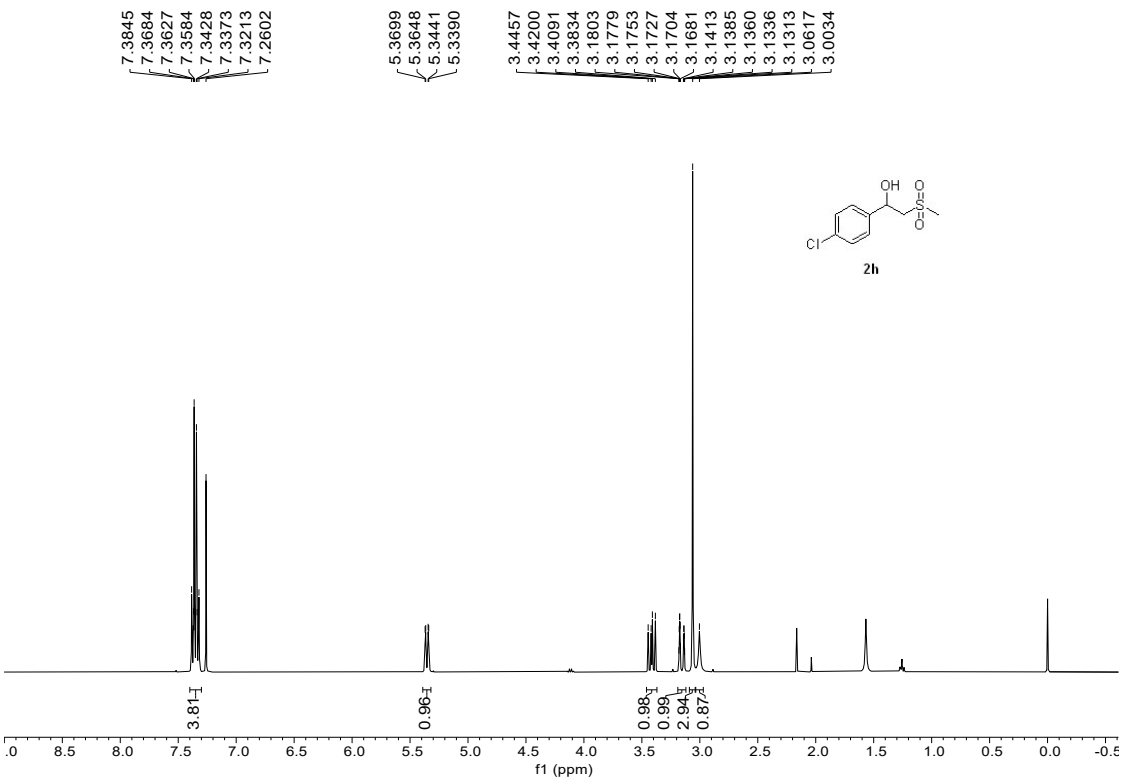


**Figure S34.** $^{1}H$ NMR spectrum of **2h** (400 MHz, in $CDCl_3$).

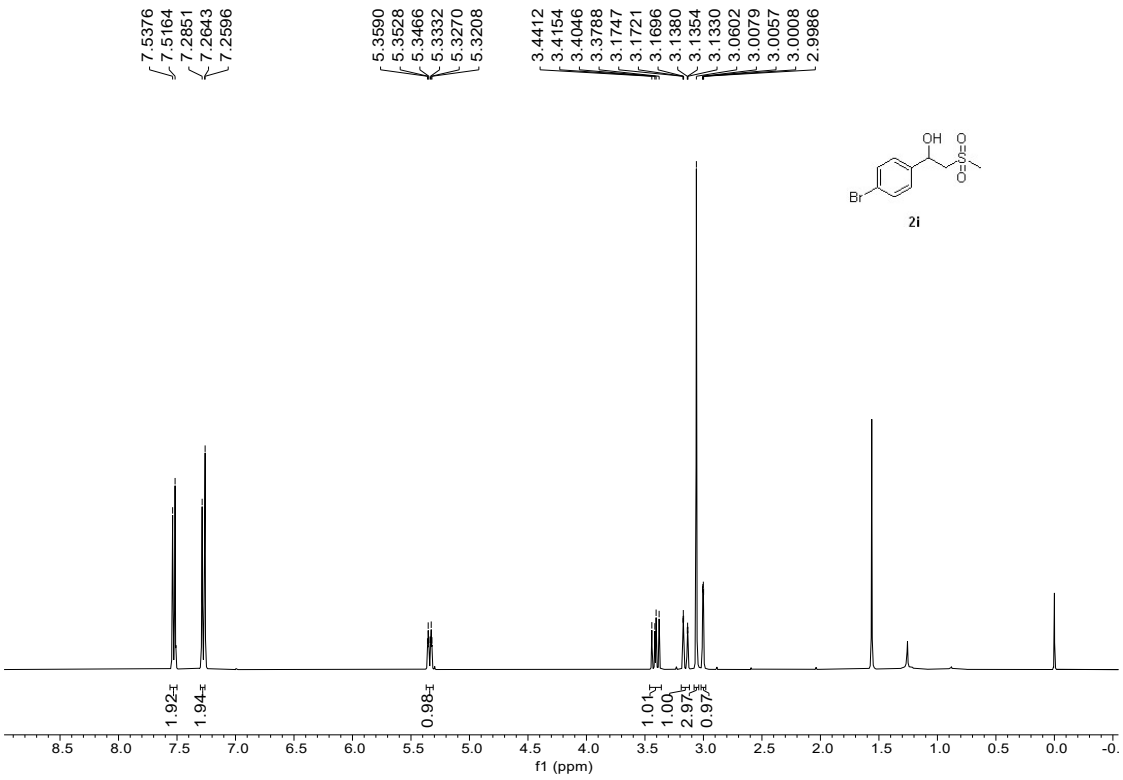


**Figure S35.** $^{1}H$ NMR spectrum of **2i** (400 MHz, in $CDCl_3$).

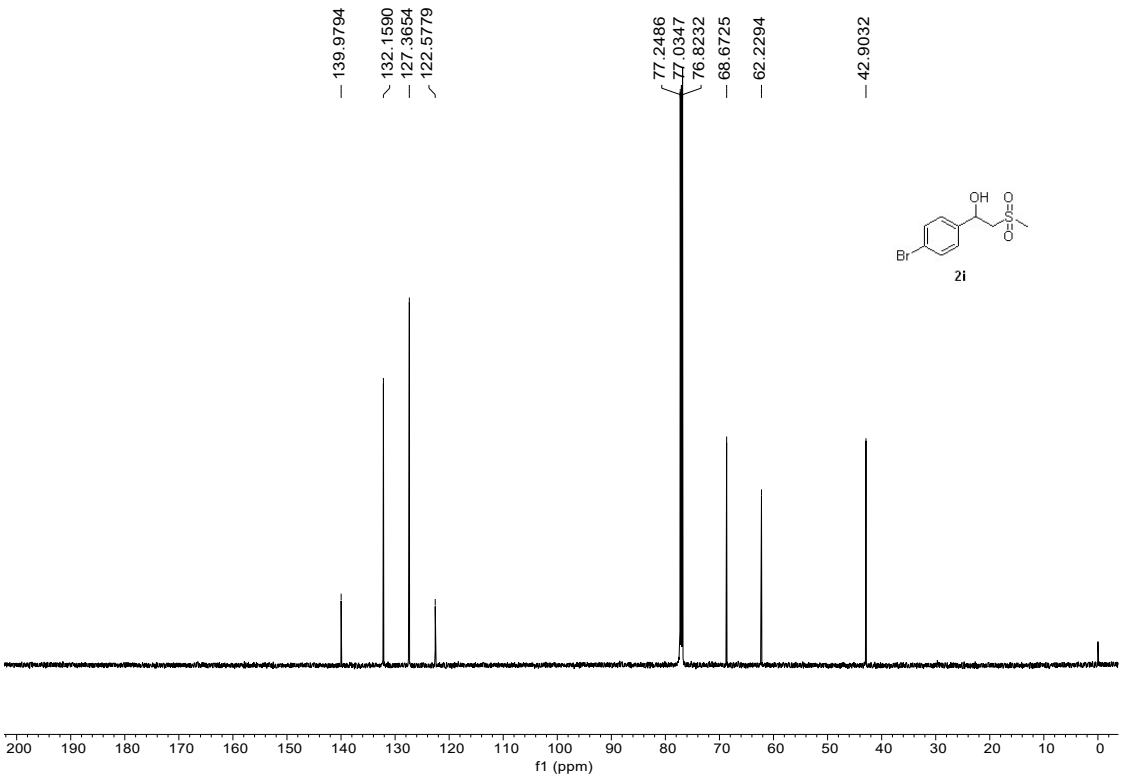

**Figure S36.** $^{13}C$ NMR spectrum of **2i** (150 MHz, in $CDCl_3$).

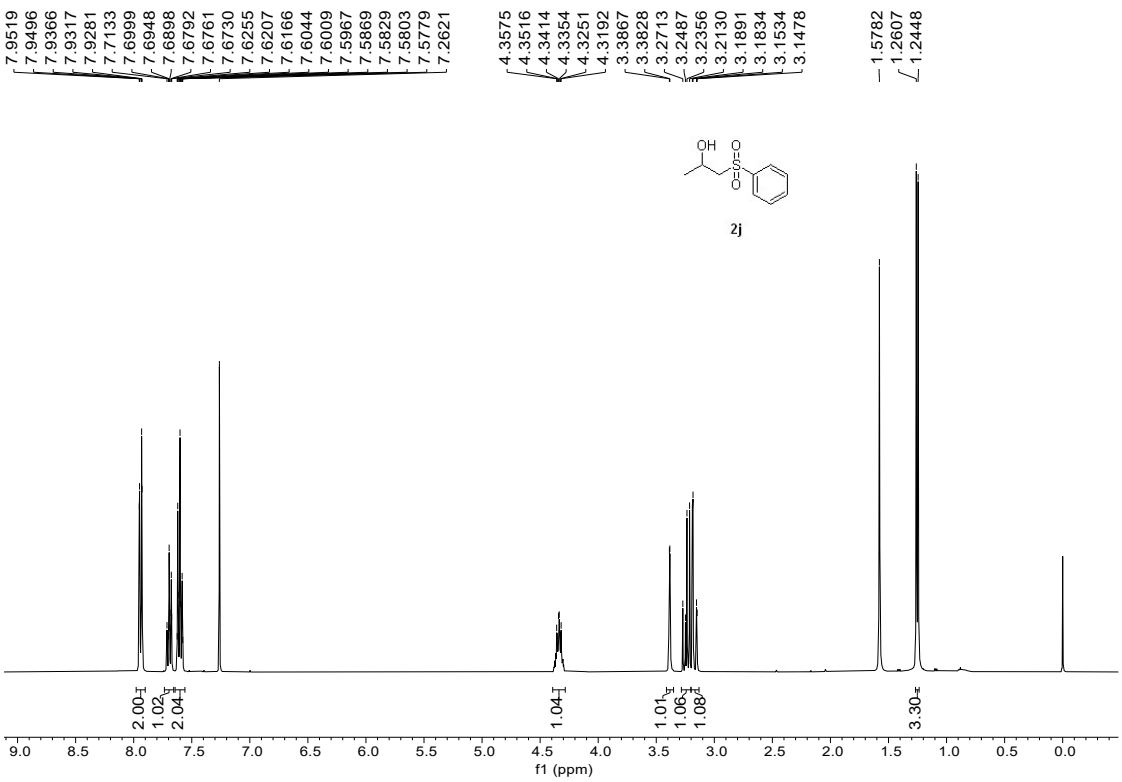


**Figure S37.** $^{1}H$ NMR spectrum of **2j** (400 MHz, in $CDCl_3$).

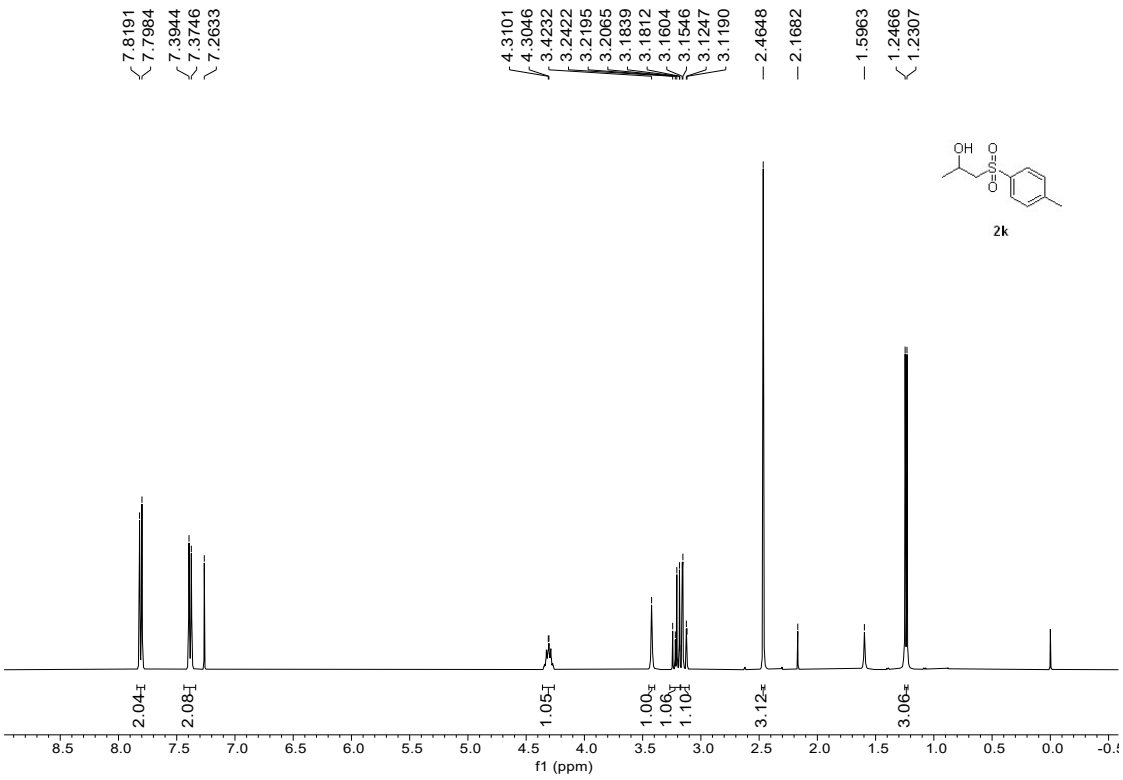


**Figure S38.** $^{1}$H NMR spectrum of **2k** (400 MHz, in $CDCl_3$).

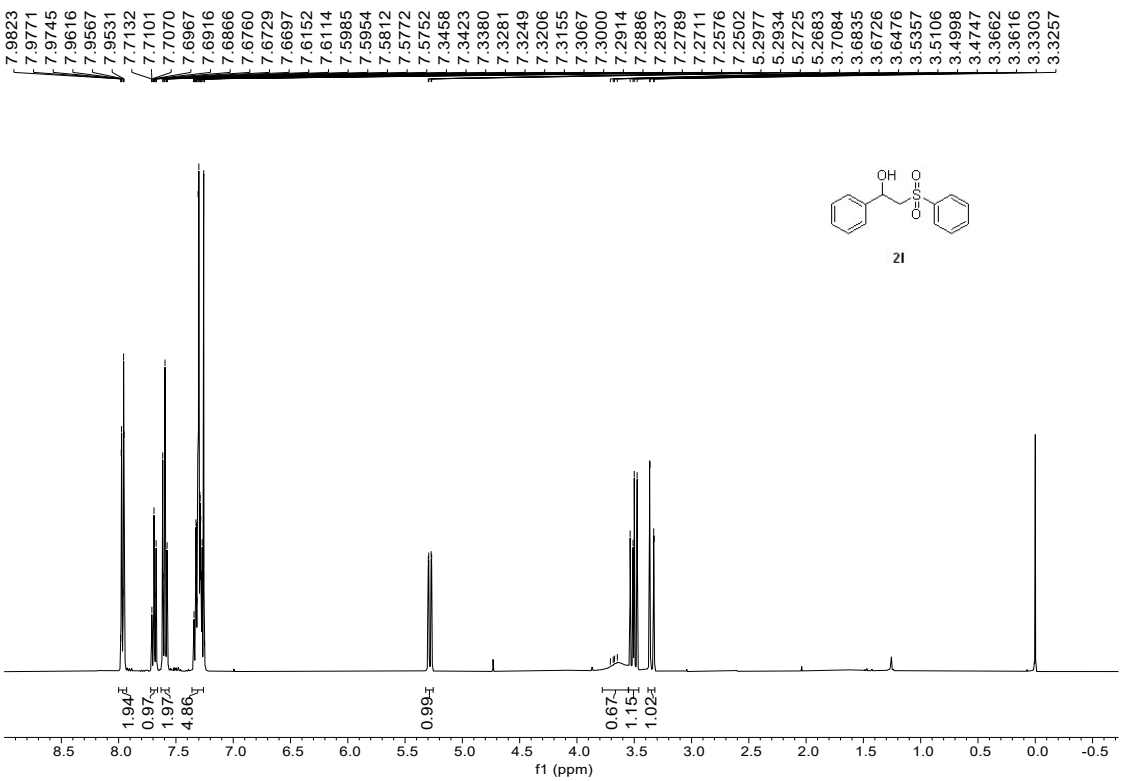


**Figure S39.** $^{1}$H NMR spectrum of **2l** (400 MHz, in $CDCl_3$).

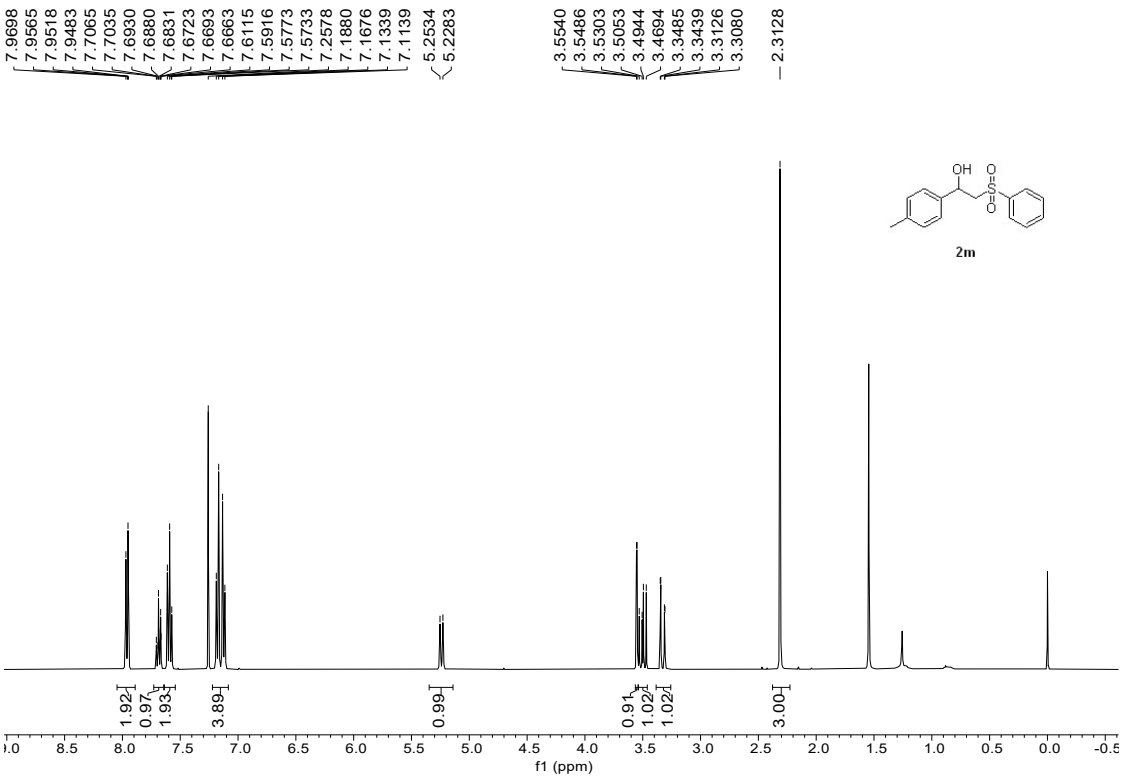


**Figure S40.** $^{1}$H NMR spectrum of **2m** (400 MHz, in $CDCl_3$).

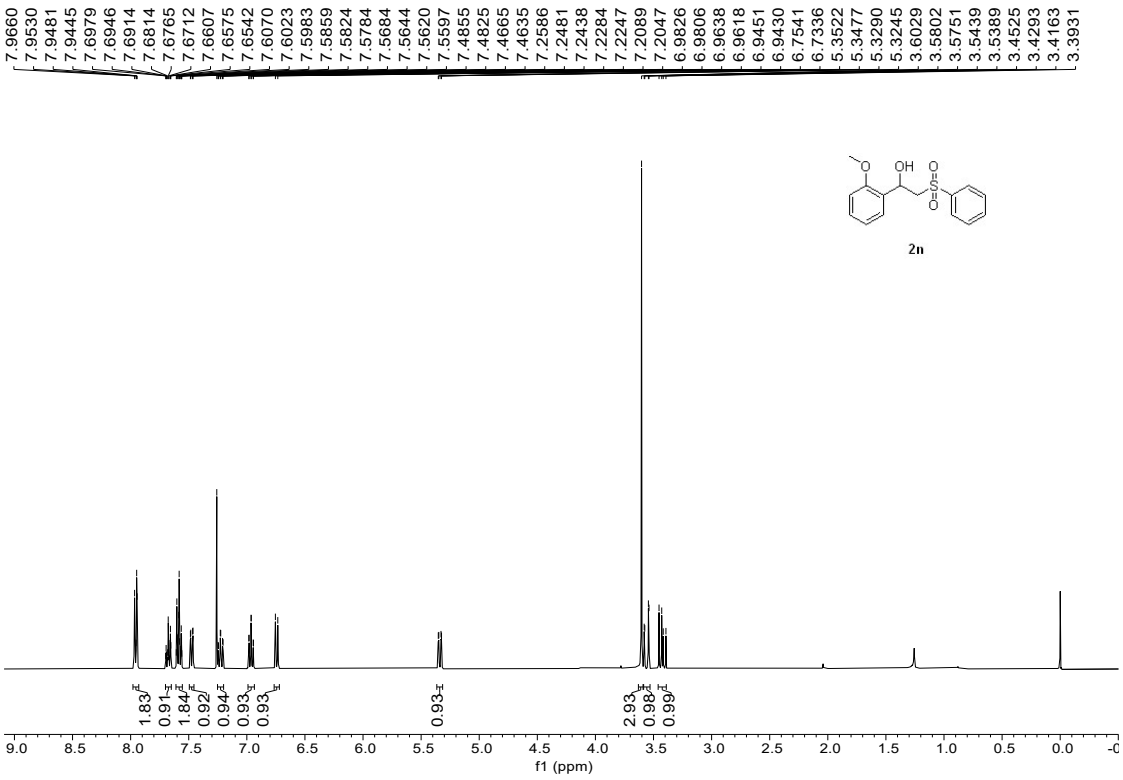


**Figure S41.** $^{1}$H NMR spectrum of **2n** (400 MHz, in $CDCl_3$).

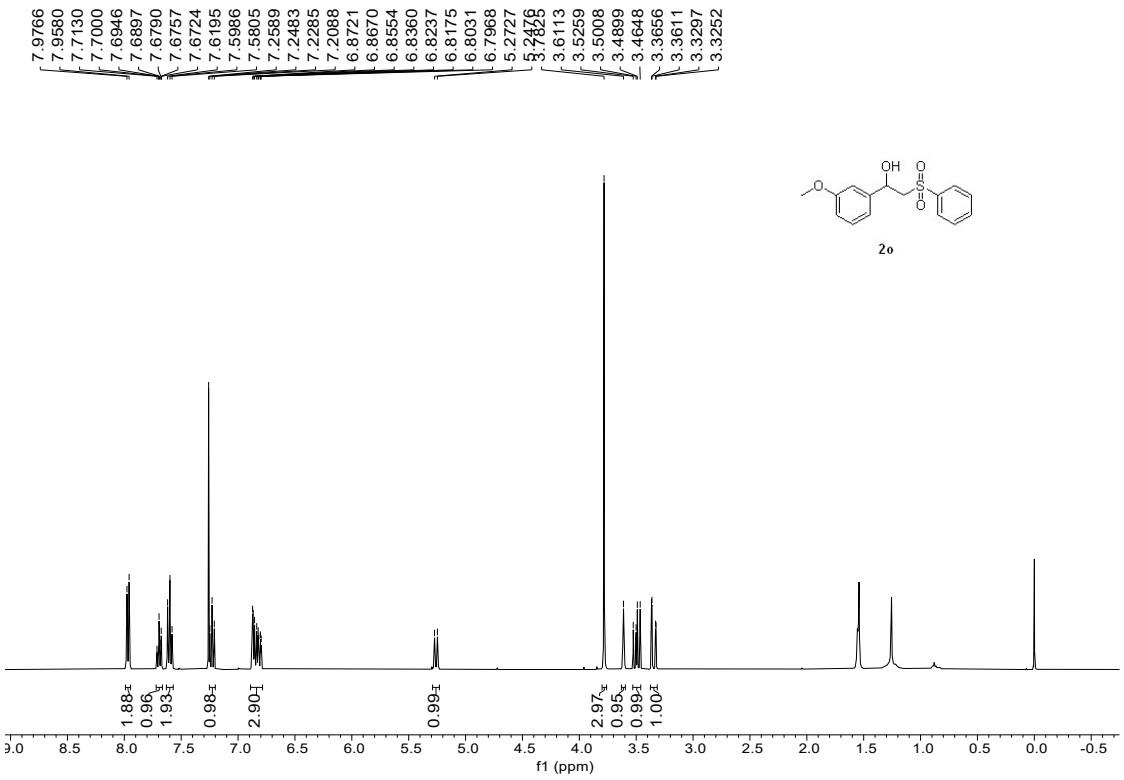


**Figure S42.** $^{1}$H NMR spectrum of **2o** (400 MHz, in $CDCl_3$).

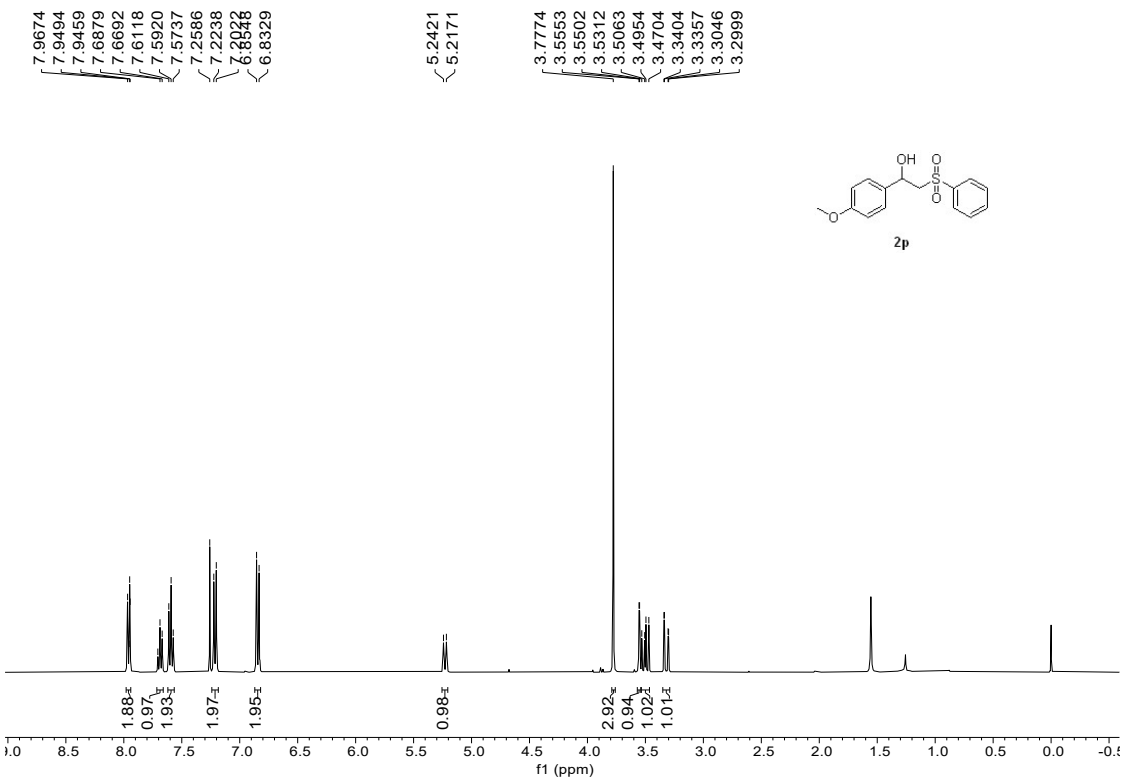


**Figure S43.** $^{1}$H NMR spectrum of **2p** (400 MHz, in $CDCl_3$).

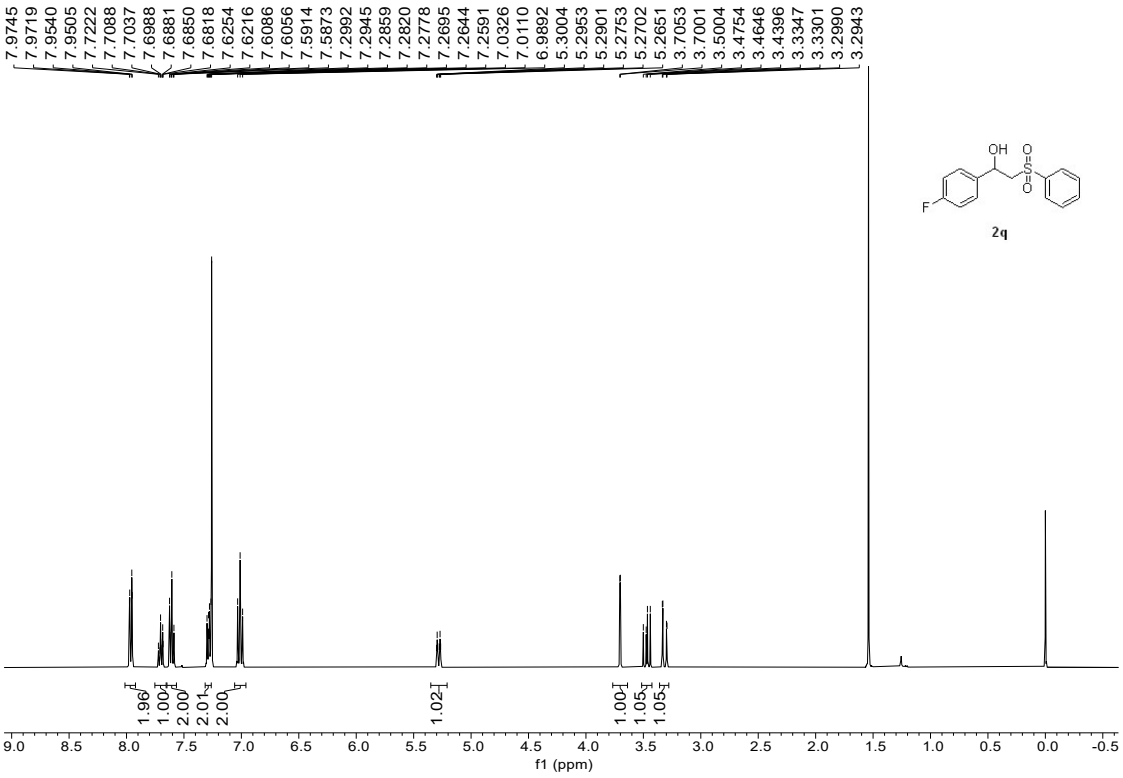


**Figure S44.** $^{1}$H NMR spectrum of **2q** (400 MHz, in $CDCl_3$).

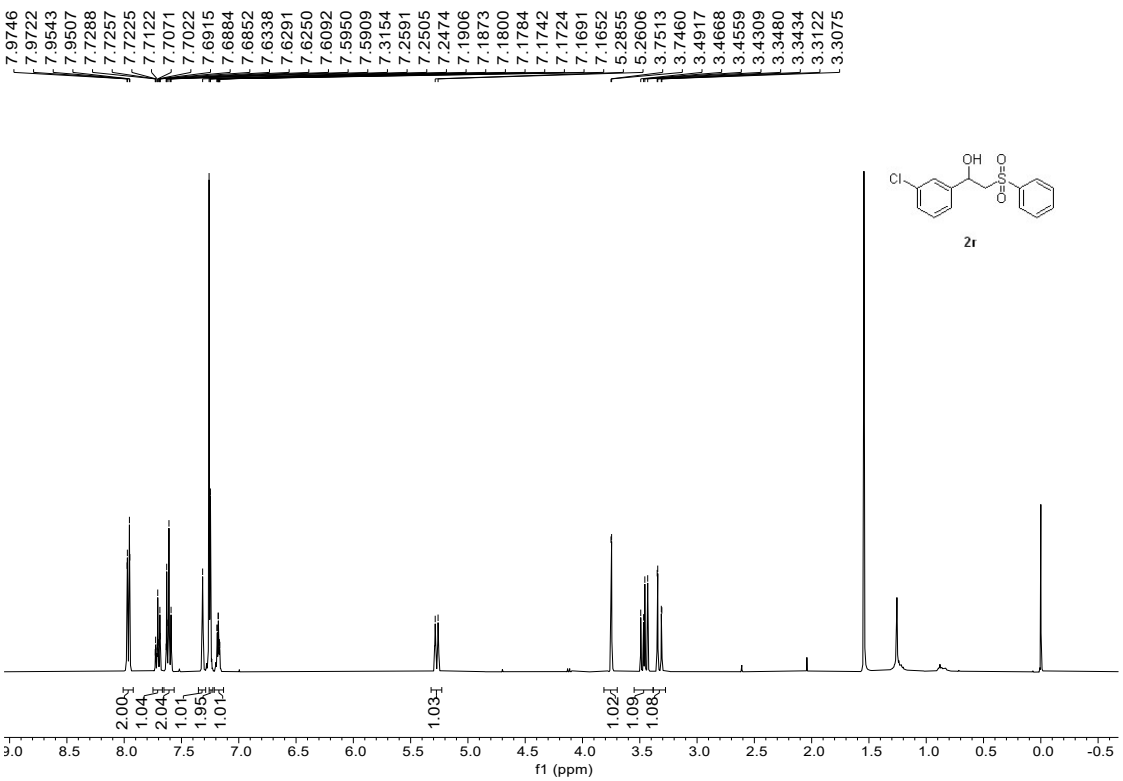


**Figure S45.** $^{1}$H NMR spectrum of **2r** (400 MHz, in $CDCl_3$).

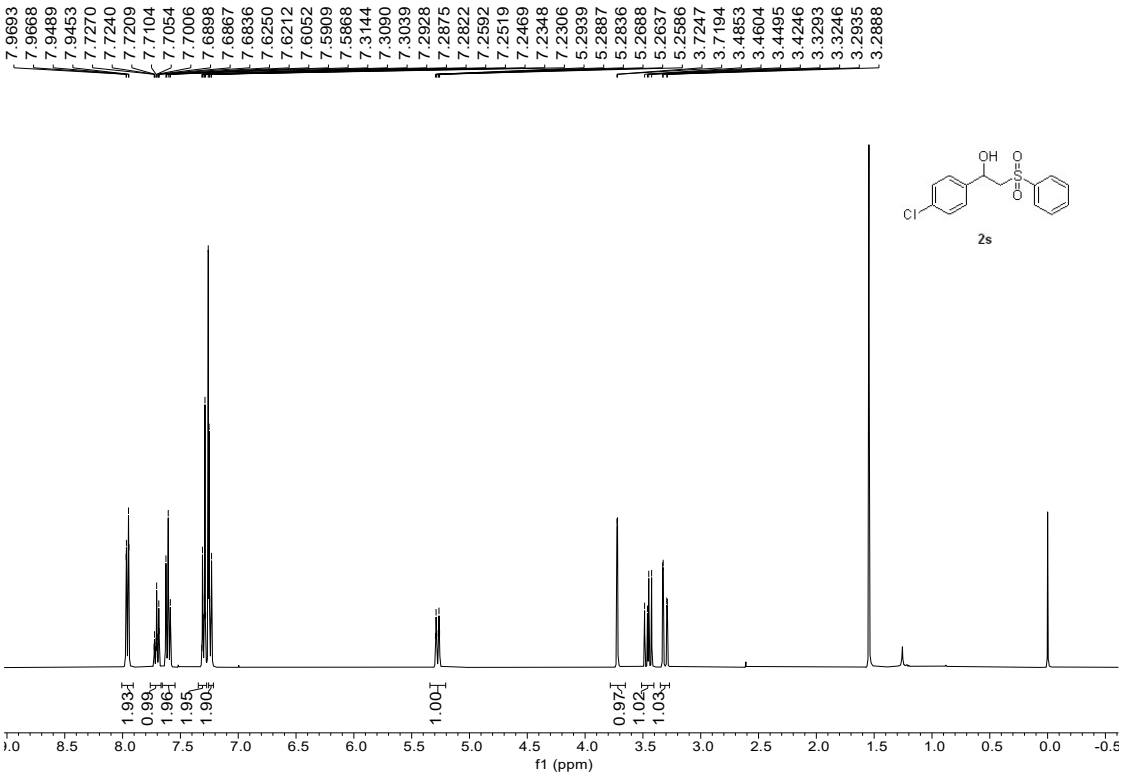


**Figure S46.** $^{1}$H NMR spectrum of **2s** (400 MHz, in $CDCl_3$).

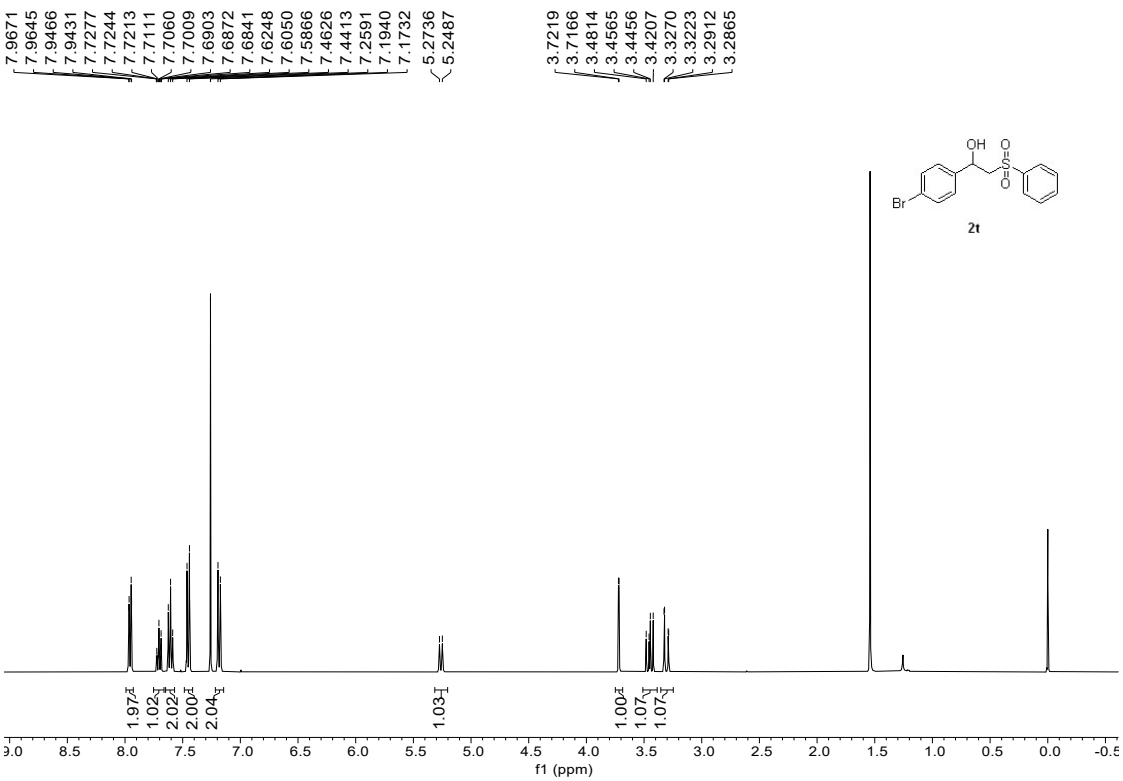


**Figure S47.** $^{1}$H NMR spectrum of **2t** (400 MHz, in $CDCl_3$).

## References


1. F. Qin, B. Qin, T. Mori, Y. Wang, L. Meng, X. Zhang, X. Jia, I. Abe and S. You, *ACS Catalysis*, 2016, **6**, 6135-6140.
2. F. Qin, B. Qin, W. Zhang, Y. Liu, X. Su, T. Zhu, J. Ouyang, J. Guo, Y. Li and F. Zhang, *ACS Catalysis*, 2018, **8**, 6012-6020.
3. L. Tao, C. Yin, X.-Q. Dong and X. Zhang, *Org. Biomol. Chem.*, 2019, **17**, 785-788.
4. K. Vega, D. Cruz, A. Oliveira, M. da Silva, T. de Lemos, M. Oliveira, R. Bernardo, J. de Sousa, G. Zanatta, F. Nasário, A. Marsaioli and M. de Mattos, *J Braz Chem Soc*, 2021, **32**, 1100-1110.
5. X. F. Huang, S. Y. Zhang, Z. C. Geng, C. Y. Kwok, P. Liu, H. Y. Li and X. W. Wang, *Adv. Synth. Catal.*, 2013, **355**, 2860-2872.
6. Q. Chen, K. Wang and C. Yuan, *New J. Chem.*, 2009, **33**, 972-975.
7. M. Biasini, S. Bienert, A. Waterhouse, K. Arnold, G. Studer, T. Schmidt, F. Kiefer, T. Gallo Cassarino, M. Bertoni, L. Bordoli and T. Schwede, *Nucleic Acids Res.*, 2014, **42**, W252-258.
8. N. H. Schlieben, K. Niefind, J. Muller, B. Riebel, W. Hummel and D. Schomburg, *J. Mol. Biol.*, 2005, **349**, 801-813.
9. P.-C. Guo, Z.-Z. Bao, X.-X. Ma, Q. Xia and W.-F. Li, *Biochimica et Biophysica Acta (BBA)-Proteins and Proteomics*, 2014, **1844**, 1486-1492.
10. O. Trott and A. J. Olson, *J. Comput. Chem.*, 2010, **31**, 455-461.
11. K. J. Bowers, D. E. Chow, H. Xu, R. O. Dror, M. P. Eastwood, B. A. Gregersen, J. L. Klepeis, I. Kolossvary, M. A. Moraes and F. D. Sacerdoti, 2006.
12. M. Lopez-Agudo, N. Rios-Lombardia, J. Gonzalez-Sabin, I. Lavandera and V. Gotor-Fernandez, *ChemSusChem*, 2021, **14**, 1-9.
13. N. Chumachenko and P. Sampson, *Tetrahedron*, 2006, **62**, 4540-4548.
14. X. Wan, Q. Meng, H. Zhang, Y. Sun, W. Fan and Z. Zhang, *Org. Lett.*, 2007, **9**, 5613-5616.